Università
Ca'Foscari
Venezia

A U.S. Transmission Model under Bayesian Specifications

Master's Degree programme in Economics and Finance - Curriculum Quantitative Economics - Ca' Foscari University - Academic Year 2022/2023

Graduand Filippo Dell'Andrea Supervisor Prof. Roberto Casarin

27 September, 2023

Abstract

This study considers the model of Miranda-Agrippino and Rey (2020) implementing the framework of Plagborg-Moller and Wolf (2021), but with various Bayesian configurations. Specifically, we use a Bayesian Structural Vector Autoregression (SVAR) approach to analyze the causal relationships between our variables. To do this, we utilize Impulse Response Functions and Forecast Error Variance Decompositions. To delve deeper into our analysis, we build a hierarchical model that incorporates both a Stochastic Volatility model and a Markov Switching model. We then proceed to compare the results obtained from these three different model specifications.

Table of contents

List of Figures

Chapter 1

Introduction

In this thesis, we replicate and extend Miranda-Agrippino and Rey (2020), implementing an original approach proposed by Plagborg-Moller and Wolf (2021). The former authors jointly evaluate the effects of financial, monetary and real variables, in the U.S. and abroad, following a 1% shock of the Federal Reserve (FED) interest rate. In particular, the authors rely on an instrumental variable to identify U.S. monetary policy shocks, building upon the framework introduced by Mertens and Ravn (2013). This approach circumvents implausible restrictions on the variable of interest. Our primary objective is to reimagine and expand upon this framework using various Bayesian specifications as an analytical exercise. Our journey begins with the development of a Bayesian Structural Vector Autoregression (SVAR) model, wherein we introduce a Hierarchical prior for the autoregressive parameter denoted as A, along with the variance-covariance matrix Σ. The foundations of Bayesian SVAR can be traced back

to the seminal work of C. A. Sims (1980), with subsequent refinements contributed by scholars such as Sims Christopher A. and Zha (1998), Canova and Gambetti (2006), Baumeister and Hamilton (2006), Canova and Ciccarelli (2009), Koop and Korobilis (2010), Bańbura, Giannone, and Reichlin (2010), and Karlsson (2013). Structural analysis, a core component of this framework, has become indispensable in economic forecasting due to its ability to shed light on how current factors shape economic trends and predictions. We develop a Bayesian framework as suggested by Litterman (1980) to address the issues of overfitting in macroeconomic data. We identify the contemporaneous effects in our model through the application of triangular restrictions, as exemplified in Christiano, Eichenbaum, and Evans (1996). Bayesian approaches offer distinct advantages over Maximum Likelihood Estimation, particularly in mitigating the overparametrization challenges inherent in VAR models. Our exploration then delves into Stochastic Volatility (SV) modeling, influenced by Jacquier, Polson, and Rossi (1994), enabling time-varying parameters within our SVAR formulation. To improve the precision of our estimates, we model error terms as time-varying, akin to Clark and Ravazzolo (2014). Pioneering works in this domain, including those by Cogley and Sargent (2005) and Primiceri (2005), have paved the way for our investigation. Recent advancements by scholars such as D'Agostino, Gambetti, and Giannone (2013) and Carriero and Clark (2016) have further enriched this field. Additionally, building upon the foundation laid by Hamilton (1989) and adopting the algorithm by Chib (1996), we extend our analysis to encompass Markov Switching (MS) models. MS models prove invaluable when there is a belief that different economic regimes and turning points influence time series data. Our approach allows us to structure the model with multiple states of the economy, aligning with prior research by Kim and

Nelson (1998), Kim and Nelson (1999), Sims Christopher A. and Zha (2006), and Sims Christopher A., Waggoner, and Zha (2008). Recent works by Billio et al. (2016), Casarin, Sartore, and Tronzano (2017), Droumaguet, Warne, and Woźniak (2017), Bianchi et al. (2019), and Lütkepohl and Woźniak (2017) have further advanced this area of study. Our most promising findings emerge from Bayesian specifications that leverage a simple Minnesota Prior and Matrix-Variate-Normal specifications, as seen in Woźniak (2016). It is essential to note, however, that we have not undertaken an exhaustive sensitivity analysis of our prior values. Given the complexity and high dimensionality of our model, the results of our Impulse Response Functions are notably sensitive to the initial choices of prior values, often yielding less insightful outcomes.

1.1 Global Factor in Risky Asset Prices

Miranda-Agrippino and Rey (2020) in the first part of the paper estimate a global factor to proxy the movement of world risky asset prices. They do so by collecting 858 prices of different risky assets traded in North America, Latin America, Europe, Asia Pacific, and Australia, from 1990 to 2012. Their method is to pick a representative market index (i.e. S&P 500) for each market at the end of 2012, including all of its components, selecting prices that allow them to cover at least 80% of cross sectional observations by 1990 and 95% in 1995. They do so to avoid over-representation of each category. They use the first difference log-priced series. With this global factor, they can explain over 20% of global risky asset price volatility in their time span. Given the small time frame and VAR analysis limitations, they estimate a global factor with commodities from the U.S., Europe, and

Japan, spanning back to 1975. This factor covers 60% of the volatility in this period. The appendix of their paper provides detailed information on this VAR estimation. To provide more intuition on this factor, the authors correlate it with some implied indexes of volatility such as the VIX (a measure of monthly expected volatility of the U.S. stock market), outlining its co-movement with common measures of market variation (in this case a negative correlation). The global factor will be used later in the impulse-response section.

1.2 Proxy-VAR with Rich-Information Bayesian VAR

In this project, we will avoid the computation of the global factor. Instead, we will concentrate on the Bayesian VAR analysis of Miranda-Agrippino and Rey (2020). The main reason why the authors studied the monetary effects of U.S. interest rate changes is that the dollar is the currency of global banking. A change in FED monetary policy affects banks' borrowing capacity, the pricing of dollar denominated assets, and cross-border capital flows on a global scale. In order to isolate its effects, the two scholars identify U.S. monetary policy shocks by exploiting 30-min price revisions around Federal Open Market Committee FOMC announcements in the fourth federal funds futures contracts (FFF4), using the techniques developed by Gürkaynak, Sack, and Swanson (2005) and Gertler and Karadi (2015). The intuition is that these futures have an average maturity of three months, and they can predict revisions of market expectations about future monetary policy one-quarter in advance. This assumption holds only if market participants can distinguish between the systematic component of policy and any observable policy action. Moreover, with asymmetrical information, the FF4 revisions

contain information about the influence of economic factors relevant to U.S. monetary policy. Policy announcements provide this information implicitly.

Chapter 2

A Bayesian VAR Framework

From Herwartz, Rohloff, and Wang (2021) we define the model as:

$$y_t = B_0^{-1}B_1 y_{t-1} + ... + B_0^{-1}B_p y_{t-p} + B_0^{-1}\varepsilon_t, t = 1, .., T, \tag{2.1}$$

$$y_t = A_j y_{t-1} + ... + A_p y_{t-p} + u_t, \tag{2.2}$$

where $j = \{1, 2, ..., p\}$ and $A(L) = B_0^{-1}B(L)$ are a $K \times N$ coefficient matrices, and L is the lag operator, and u_t in (2.2) is serially uncorrelated with zero mean and positive definite (non-diagonal) covariance matrix Σ_u. The structural shocks ε_t in the second reduced form are assumed to be mutually uncorrelated and normalised to have unit variance. $\Xi(\varepsilon_t \varepsilon_t') = I_K$. Structural shocks are mapped to the reduced-form system through a K x K non-singular matrix B_0, such that $B_0^{-1}B_0^{-1'} = \Sigma_u$. For

simplicity, the process is assumed to be causal and $\det A(z) = \det(I_k - \sum_{j=1}^{p} A_j z^j) \neq 0$ for $|z| \leq 1$. This ensures that the process has a Wold moving average MA representation. Moreover,

$$y_t = \mu + \sum_{i=0}^{\infty} \Phi_i u_{t-i} = \mu + \sum_{i=0}^{\infty} \Phi_i B_0 \varepsilon_{t-i} = \mu + \sum_{i=0}^{\infty} \Theta_i \varepsilon_{t-i} \tag{2.3}$$

with

$$\mu = A(1)^{-1}\nu, \quad \Phi_0 = I_K, \ \Phi_i = \sum_{j=1}^{i} A_j \Phi_{i-j}, \quad A_j = 0 \ for \ j > p. \tag{2.4}$$

The MA representation in Eq. (2.3) is of particular importance because the structural MA coefficients $\Theta_i = \Phi_i B_0$ cannot be recovered without a proper identification. We will briefly outline the Proxy SVAR approach.

Let z_t be an external instrument to identify the structural shock of interest ε_{kt}, $\forall k \ in \ \{1, \dots, K\}$. z_t has to satisfy the *relevant* condition $\Xi(\varepsilon_{kt} z_t) = \phi \neq 0$ and the *exogeneity* condition $\Xi(\varepsilon_{lt} z_t) = 0, \forall l \, \epsilon \, \{1, \dots, K\} \setminus \{k\}$.

From these conditions, it follows that the population covariances between the instrument and VAR

residuals obtain the k-th column B_0, denoted by B_{0k}, are:

$$\begin{aligned} \Xi(u_t z_t) &= B_{0,k}, \\ \Xi(\varepsilon_{kt} z_t) &= \phi B_{0,k}. \end{aligned} \tag{2.5}$$

Moreover, let π denotes the 1xK coefficient vector from the regression of the instrument on the residual vector u_t gives the shock ε_{kt} up to a scale ϕ. $\pi u_t = \Xi(z_t u_t^{'})\Sigma_u^{-1} u_t = \phi B_{0,k}^{'}\left[B_0 B_0^{'}\right] u_t = \phi e_t^{'}\varepsilon_{kt}$. Plagborg-Moller and Wolf (2021), exploiting their result that Local Projections and VAR impulse response function are equal up to a constant of proportionality and show that proxy SVARs impulse responses can be computed by putting the instrument in the first row of the data vector y_t in a SVAR framework. This result follows from the invertibility of ε and two assumptions: the data y_t is covariance-stationary and a jointly Gaussian vector time series.

In our Bayesian approach, these requirements are met when we define the distributions of our error terms and prior specifications. We will outline them in the next section.

2.1 A Linear VAR Model

We specify our model as Woźniak (2016) that is:

$$\begin{aligned} Y &= XA + E, \\ E|X &\sim MN_{T\times N}(0_{T\times N}, \Sigma, I_T), \end{aligned} \tag{2.6}$$

where $MN_{T\times N}(A, \Sigma, \Sigma_a)$ denotes a matrix-variate normal distribution with location A, and scales Σ and Σ_a. Given that the function Y is a linear combination of the error terms E, we can write (2.6) as

$$Y|X, A \sim MN_{T\times N}(XA, \Sigma, I_T). \tag{2.7}$$

Hence, the Likelihood function follows a Matrix-Variate-Normal form:

$$L(A, \Sigma|Y, X) \propto \det(\Sigma)^{-\frac{T}{2}} \exp\left\{-\frac{1}{2} tr\left[\Sigma^{-1}(Y - XA)'(Y - XA)\right]\right\}$$

$$\propto \det(\Sigma)^{-\frac{T}{2}} \left\{-\frac{1}{2} tr\left[\Sigma^{-1}(A - \hat{A})'X'X(A - \hat{A})\right]\right\}$$

$$\exp\left\{-\frac{1}{2} tr\left[\Sigma^{-1}(Y - X\hat{A})'(Y - X\hat{A})\right]\right\},$$

that can be presented as a Normal-Inverse Wishart distribution for (A, Σ).

$$L(A, \Sigma|Y, X) = \mathcal{NIW}_{K\times N}\left(\hat{A}, (X'X)^{-1}, (Y - X\hat{A})'(Y - X\hat{A}), T - N - K - 1\right), \tag{2.8}$$

where

$$\begin{aligned} \hat{A} &= (X'X)^{-1}X'Y, \\ \hat{\Sigma} &= \frac{1}{T}(Y - X\hat{A})'(Y - X\hat{A}) \end{aligned} \tag{2.9}$$

are the Maximum Likelihood Estimation estimator of A and Σ, respectively. In the basic model, our

prior distribution follows a natural-conjugate prior distribution of the same form:

$$\begin{aligned} p(A, \Sigma) &= p(A|\Sigma)p(\Sigma), \\ A|\Sigma &\sim MN_{K\times N}(\underline{A}, \Sigma, \underline{V}), \\ \Sigma &\sim IW_N(\underline{S}, \underline{\nu}) \end{aligned} \tag{2.10}$$

with parameters:

$$\underline{A} = [0_{1\times N} \quad I_N \quad 0_{N\times(p-1)N}]', \tag{2.11}$$

$$Var[vec(A)] = \Sigma \otimes \underline{V}, \tag{2.12}$$

$$\underline{V} = diag([\kappa_2 \quad \kappa_1(p^{-2} \otimes I_N)]) \tag{2.13}$$

with

$$p = [1, 2, ...P],$$

where $\underline{V}$ represents the Minnesota prior firstly introduced by Doan, Sims, and Litterman (1984) and Litterman (2020), and κ_2 and κ_1 describe, respectively, the priors of the overall shrinkage level of the constant term and the variance-covariance matrix of the autoregressive slopes for the constant term. We specify $\kappa_2 = 1$ and $\kappa_1 = 0.02$ to respect Plagborg-Moller and Wolf (2021) assumptions. Moreover, we set the prior of the autoregressive parameters A equal to a vector of zeros. The resulting full

conditional posterior is:

$$\begin{aligned} p(A,\Sigma|Y,X) &= p(A|Y,X,\Sigma)p(\Sigma|Y,X), \\ p(A|Y,X,\Sigma) &= MN_{K\times N}(\bar{A},\Sigma,\bar{V}), \\ p(\Sigma|Y,X) &= IW_N(\bar{S},\bar{\nu}). \end{aligned} \tag{2.14}$$

We can derive the full conditional posterior:

$P(A,\Sigma|Y,X) \propto L(A,\Sigma|Y,X)p(A,\Sigma) \propto L(A,\Sigma|Y,X)p(A|\Sigma)p(\Sigma) \propto$

$$\det(\Sigma)^{-\frac{T}{2}} \times \exp\left\{-\frac{1}{2}tr\left[\Sigma^{-1}(A-\widehat{A})'X'X(A-\widehat{A})\right]\right\} \times \exp\left\{-\frac{1}{2}tr\left[\Sigma^{-1}(Y-X\widehat{A})'(Y-X\widehat{A})\right]\right\}$$

$$\times \det(\Sigma)^{-\frac{N+K+\underline{\nu}+1}{2}} \times \exp\left\{-\frac{1}{2}tr\left[\Sigma^{-1}(A-\underline{A})'\underline{V}^{-1}(A-\underline{A})\right]\right\} \times \exp\left\{-\frac{1}{2}tr\left[\Sigma^{-1}\underline{S}\right]\right\}.$$

After some calculations we obtain:

$p(A,\Sigma|Y,X) \propto$

$$\det(\Sigma)^{-\frac{T+N+K+\underline{\nu}+1}{2}} \times \exp\left\{-\frac{1}{2}tr\left[\Sigma^{-1}\left[(A-\bar{A})'\bar{V}^{-1}(A-\bar{A})+\underline{S}+Y'Y+\underline{A}'\underline{V}^{-1}\underline{A}-\bar{A}'\bar{V}^{-1}\bar{A}\right]\right]\right\},$$

where the full conditional posterior has the same natural-conjugate form of our prior:

$$\begin{aligned} p(A,\Sigma|Y,X) &= p(A|Y,X,\Sigma)p(\Sigma|Y,X), \\ p(A|Y,X,\Sigma) &= MN_{K\times N}(\bar{A},\Sigma,\bar{V}), \\ p(\Sigma|Y,X) &= IW_N(\bar{S},\bar{\nu}) \end{aligned} \tag{2.15}$$

with posterior parameters:

$$\bar{V} = (X'X + \underline{V}^{-1})^{-1}, \tag{2.16}$$

$$\bar{A} = \bar{V}(X'Y + \underline{V}^{-1}\underline{A}), \tag{2.17}$$

$$\bar{\nu} = T + \underline{\nu}, \tag{2.18}$$

$$\bar{S} = \underline{S} + Y'Y + \underline{A}'\underline{V}^{-1}\underline{A} - \bar{A}'\bar{V}^{-1}\bar{A}. \tag{2.19}$$

In order to compute our posterior parameters in R, we first specify values for our priors, then calculate the posteriors and draw A and Σ respectively from Matrix-Variate-normal and Inverse Wishart distributions. At this point, we can obtain our structural parameters through a Cholesky decomposition of our matrix Σ, namely with $\Sigma^{-1} = (B_0 B_0')$.

2.2 A Bayesian Hierarchical Model

In the hierarchical model, we set hyperprior parameters for the autoregressive parameter κ_A to follow an Inverse Gamma 2 distribution $IG2(\underline{S}_\kappa, \underline{\nu}_\kappa)$ and κ_Σ hyperprior parameter for the variance-covariance matrix to follow a Gamma Distribution $G(\underline{S}_\Sigma, \underline{a}_\Sigma)$. We define a hierarchical model to provide flexibility and reduce uncertainty in our model. We will define the full conditional posterior of the hyperparameter κ_A first.

$$p(\kappa_A|A,\Sigma,Y,X) \propto L(Y|X,A,\Sigma) \times p(\kappa_A) \times p(A|\Sigma,\kappa_A) \times p(\Sigma|\kappa_A) \propto p(\kappa_A) \times p(A|\Sigma,\kappa_A)$$

$$\propto (\kappa_A)^{-\frac{\underline{\nu_a}\kappa_A{}^{+2}}{2}} \exp\left\{-\frac{1}{2}\frac{\underline{s_a}}{\kappa_A}\right\} \times \exp\left\{-\frac{1}{2} tr\left[\Sigma^{-1}(A-\underline{A})'\frac{1}{\kappa}(\underline{V_\kappa})^{-1}(A-\underline{A})\right]\right\} \times \det(\kappa_A \underline{V})^{-\frac{N}{2}}$$

$$\propto (\kappa_A)^{-\frac{\underline{\nu_a}\kappa_A{}^{+2+NK}}{2}} \exp\left\{-\frac{1}{2}\frac{1}{\kappa_A}\left[\underline{s_a}_{\kappa_A} + tr\left[\Sigma^{-1}(A-\underline{A})'\underline{V}^{-1}(A-\underline{A})\right]\right]\right\},$$

where we recognise the kernel of an Inverse Gamma 2 Distribution with parameters:

$$\bar{s}_a = \underline{s}_a + tr\left[\Sigma^{-1}(A-\underline{A})'\underline{V}^{-1}(A-\underline{A})\right], \tag{2.20}$$

$$\bar{\nu}_a = \underline{\nu}_a + NK. \tag{2.21}$$

In addition, we obtain a similar full conditional posterior of the hyperparameter κ_Σ.

$$p(\kappa_\Sigma|A,\Sigma,Y,X) \propto L(Y|X,A,\Sigma) \times p(\kappa_\Sigma) \times p(A|\Sigma,\kappa_A) \times p(\Sigma|\kappa_\Sigma) \times p(\kappa_A)$$

$$\propto p(\kappa_\Sigma) \times p(\Sigma|\kappa_\Sigma)$$

$$\propto (\kappa_\Sigma)^{-\frac{\nu N}{2}} \exp\left[-\frac{1}{2}\frac{\kappa_\Sigma}{tr\left[\Sigma^{-1}\underline{s}_\Sigma\right]^{-1}}\right] \times (\kappa_\Sigma)^{\underline{a}_\Sigma - 1} \exp\left[-\frac{\kappa_\Sigma}{\underline{s}_\Sigma}\right]$$

$$\propto (\kappa_\Sigma)^{\frac{N\underline{\nu}+2\underline{a}_\Sigma-2}{2}} \exp\left[-\frac{\kappa_\Sigma}{\left[2tr\left[\Sigma^{-1}\underline{s}_\Sigma\right]^{-1} + \left[\underline{s}_\Sigma\right]^{-1}\right]^{-1}}\right],$$

where we can recognise the kernel of a Gamma Distribution with parameters

$$\bar{s}_\Sigma = \left[2\left[tr\Sigma^{-1}\underline{s}_\Sigma\right]^{-1} + \left[\underline{s}_\Sigma\right]^{-1}\right]^{-1}, \tag{2.22}$$

$$\bar{a}_\Sigma = \frac{N\underline{\nu}}{2} + \underline{a}_\Sigma. \tag{2.23}$$

Therefore, our new full conditional posterior distribution will be as follows:

$$p(A,\Sigma|X,Y,\kappa_A,\kappa_\Sigma) \propto L(A,\Sigma|Y,X) \times p(A|\Sigma,\kappa_A) \times p(\Sigma|\kappa_\Sigma)$$

$$\propto \det(\Sigma)^{-\frac{K}{2}} \exp\left\{-\frac{1}{2} tr\left[\Sigma^{-1}(Y-XA)'(Y-XA)\right]\right\}$$

$$\times \exp\left\{-\frac{1}{2} tr\left[\Sigma^{-1}(A-\underline{A})'(\kappa_A \underline{V})^{-1}(A-\underline{A})\right]\right\}$$

$$\times \det(\Sigma)^{\frac{\underline{\nu}+N+1}{2}} \exp\left\{-\frac{1}{2} tr\left[\Sigma^{-1}\kappa_\Sigma\right]\right\}.$$

We recognize the kernel of a matrix-normal inverse Wishart distribution, with parameters as follows:

$$\bar{V} = (X'X + (\kappa_A \underline{V}))^{-1}, \tag{2.24}$$

$$\bar{A} = \bar{V}(X'Y + (\kappa_A \underline{V}^{-1}\underline{A})), \tag{2.25}$$

$$\bar{S} = I_N \kappa_\Sigma + Y'Y + \underline{A}'(\kappa_A \underline{V})^{-1}\underline{A} - \bar{A}'\bar{V}^{-1}\bar{A}, \tag{2.26}$$

$$\bar{\nu} = T + \underline{\nu}. \tag{2.27}$$

2.2.1 Posterior Approximation

In order to reach our analytical solutions we update our Gibbs Sampler procedure with an additional step. We generate random draws from the joint posterior distribution and update them at each iteration to compute our posterior distribution parameters. In our case, we exploit the following procedure: initialize κ_A and κ_Σ at $\kappa_A^{(0)}$ and $\kappa_\Sigma^{(0)}$. We input starting values following Giannone, Lenza, and Primiceri (2015).

At each iteration i:

1. Draw $(A,\Sigma)^{(i)} \sim p(A,\Sigma \| X,Y,\kappa_A^{(i-1)},\kappa_\Sigma^{(i-1)})$;

2. Draw $\kappa_A^{(i)} \sim p(\kappa_A|Y, X, A, \Sigma)$;

3. Draw $\kappa_\Sigma^{(i)} \sim p(\kappa_\Sigma|Y, X, A, \Sigma)$.

Repeat steps 1 and 2 for $(S_1 + S_2)$ times. Discard the first S_1 repetitions. Return the output as $\left\{A^{(i)}, \Sigma^{(i)}\right\}_{i=S_1+1}^{S_2}$.

2.3 A Bayesian Stochastic Volatility Extension

We present an alternative Bayesian model where the conditional heteroskedasticity of the error terms follows a dynamic model (Jacquier, Polson, and Rossi (1994)). Further developments of this kind of framework include Jacquier, Polson, and Rossi (2004). We apply the auxiliary ten-mixture approach of Omori et al. (2007) and the precision sampling of Chan and Jeliazkov (2009).

$$Y = XA + E, \tag{2.28}$$

$$E|X \sim MN_{T\times N}(0_{T\times N}, diag(\sigma^2)), \tag{2.29}$$

where

$$\sigma^2 = \{\exp(h_1), ..., \exp(h_T)\},$$

and each h_t is obtained from a Stochastic Volatility model

$\tilde{y} = h + \tilde{\epsilon}$,

$Hh = h_0 e_{1.T} + \sigma_v v$,

$\tilde{\epsilon}|s \sim \mathcal{N}_T(\mu_s, diag(\sigma_s^2))$,

$v \sim \mathcal{N}_T(0_T, I_T)$,

where s, μ_s, and σ_2^s, are $T \times 1$ vectors. The hierarchical prior is given by

$$p(h, s, h_0, \sigma_v^2) = p(h|h_0, \sigma_v^2)p(h0)p(\sigma_v^2)p(s), \tag{2.30}$$

and the prior distribution of $h|h_0, \sigma_v^2$ is given by

$p(h|h_0, \sigma_v^2) \sim \mathcal{N}_t(h0H^{-1}e_{1.T}, \sigma_v^2(H'H)^{-1})$

$\propto \det(\sigma_v^2 I_T)^{-\frac{1}{2}} \exp\left\{-\frac{1}{2}\frac{1}{\sigma_v^2}(Hh - h_0 e_{1.T})'(Hh - h_0 e_{1.T})\right\}$

The marginal priors are

$$p(h_0) = \mathcal{N}(0, \underline{\sigma}_h^2), \tag{2.31}$$

$$p(\sigma_v^2) = \mathcal{IG}2(\underline{s}, \underline{\nu}), \tag{2.32}$$

$$p(s_t) = \mathcal{M}ultinomial(m_{m=1}^{10}, Pr(s_t = m)_{m=1}^{10}). \tag{2.33}$$

Combining the priors with the conditional likelihood

$$\exp\left\{-\frac{1}{2}(h - (\tilde{y} - \mu_s)'diag(\sigma_s^2)^{-1}(h - (\tilde{y} - \mu_s))\right\},$$

we obtain the full conditional posterior of $h|y, s, h_0, \sigma_v^2 \sim \mathcal{N}_T(\bar{h}, \bar{V}_h)$ with parameters:

$$\bar{H}_h = \left[diag(\sigma_s^2)^{-1} + \sigma_v^{-2} H'H\right]^{-1}, \tag{2.34}$$

$$\bar{h} = \bar{V}_h \left[diag(\sigma_s^2)^{-1}(\tilde{y} - \mu_s) + \sigma_v^{-2} h_0 e_{1.T}\right]. \tag{2.35}$$

In addition, incorporating the results from the posterior distributions of h, s, σ_v^2, and h_0, we obtain the updated parameters of the full conditional posterior of our Matrix-Variate-normal and Inverse Wishart distribution:

$$\bar{V} = (X' diag(\sigma^2)^{-1} X + (\kappa_A \underline{V}))^{-1}, \tag{2.36}$$

$$\bar{A} = \bar{V}(X' diag(\sigma^2)^{-1} Y + (\kappa_A \underline{V}^{-1} \underline{A})), \tag{2.37}$$

$$\bar{S} = I_N \kappa_\Sigma + Y' diag(\sigma^2)^{-1} Y + \underline{A}^{'} (\kappa_A \underline{V})^{-1} \underline{A} - \bar{A}^{'} \bar{V}^{-1} \bar{A}, \tag{2.38}$$

$$\bar{\nu} = T + \underline{\nu}. \tag{2.39}$$

In this model - and also in the Markov Switching case - we use posterior mean values of κ_A and κ_Σ of the hierarchical model as initial values of the κs

2.3.1 Posterior Approximation

Based on the previous model, we can update the Gibbs sampler. Initialize σ^2, κ_A and κ_Σ at $\sigma^{2(0)}$ $\kappa_A^{(0)}$ and $\kappa_\Sigma^{(0)}$.

At each iteration i:

1. Draw $(A, \Sigma)^{(i)} \sim p(A, \Sigma \| X, Y, \kappa_A^{(i-1)}, \kappa_\Sigma^{(i-1)}, \sigma^{2(i-1)})$;
2. Draw $(\sigma^2)^{(i)} \sim p(h|y, s, h_0, \sigma_v^2)$;
3. Draw $\kappa_A^{(i)} \sim p(\kappa_A|Y, X, A^{(i)}, \Sigma^{(i)})$;
4. Draw $\kappa_\Sigma^{(i)} \sim p(\kappa_\Sigma|Y, X, A^{(i)}, \Sigma^{(i)})$.

Repeat steps 1 and 2 for $(S_1 + S_2)$ times. Discard the first S_1 repetitions. Return the output as $\left\{A^{(i)}, \Sigma^{(i)}, \kappa_A^{(i)}, \kappa_\Sigma^{(i)}, (\sigma^2)^{(i)}\right\}_{i=S_1+1}^{S_2}$.

2.4 Bayesian Markov Switching

We present a final extension using a Markov Switching (MS) model. We make a brief presentation of MS models using Song and Woźniak (2021), Frühwirth-Schnatter (2006), and Hamilton (1994). The first MS model applied in autoregressive economic model is the one of Hamilton (1989), who finds that with two regimes GNP data follow closely NBER recession dates. In our model, we similarly assume two states $s_t = \{1, 2\}$ where we constrain the autoregressive parameter such that $\bar{\Sigma}^{up} > \bar{\Sigma}^{down}$. The transition probability is $P = [p_{ij}]_{KxK}$, $i, j = \{1, 2\}$ that is the probability of going from state i to state j, where $\sum_j^K p_{ij} = 1$. In our case, $K = 2$. s_t is an irreducible, aperiodic Markov Chain that starts from its ergodic distribution. Irreducibility implies that $\forall i, j \in \mathbf{S}, \exists t \geq 0 : P(s_t = i|s_{t-1} = j) > 0$. Aperiodicity states that $gcd\{P(s_t = i|s_{t-1} = j) > 0\} = 1$, where gcd is the greatest common divisor. We can solve for the invariant (ergodic) probabilities η from $p'\eta = \eta$. Solving for $K = 2$ we obtain

$\eta_1 = \frac{p_{21}}{p_{21}+p_{12}}$ and $\eta_2 = \frac{p_{12}}{p_{21}+p_{12}}$. We first derive a MS model where the states are exogenously given, namely

$$s_t = \begin{cases} 1 \text{ if } t \in \text{ High Volatility} \\ 2 \text{ if } t \in \text{ Low Volatility} \end{cases} \tag{2.40}$$

We determine periods of high volatility by identifying outliers using a method developed by Chen and Liu (1993), which involves using the R package `tso` applied to our estimated variance (σ^2) in the Stochastic Volatility model. Then, we utilize the results obtained from the posterior mode of the intercept terms of $\bar{A}^{up}$ and $\bar{A}^{down}$ as initial parameters for the intercepts of $\underline{A}^{up}$ and $\underline{A}^{down}$ in the subsequent endogenous model that I will explain later. Previous works that use results from previously estimated models as priors for the model of interest are Del Negro and Schorfheide (2004) and Ciccarelli and García (2021). The endogenous Markov Switching (MS) model we are introducing is similar to the extended hierarchical model, but it differs in that it now accounts for two distinct regimes, and we need to compute the transition probability matrix to describe these regimes. Given a Beta prior for p_{ij} $p(p_{ii}, 1-p_{ii}) \sim Be(\underline{\tau_{ij}}, \underline{\tau_{ij}})$ with $i, j = \{1, 2\}$, one gets the following:

$$p(A(s_t), \Sigma(s_t), s_t, p_{11}, p_{22} | X(s_t), Y(s_t), \kappa_A(s_t), \kappa_\Sigma(s_t)) \propto$$

$$L(A(s_t), \Sigma(s_t), s_t, , p_{11}, p_{22} | Y(s_t), X(s_t)) \times$$

$$p(A(s_t), s_t | \Sigma(s_t), \kappa_A(s_t), p_{11}, p_{22}) \times p(\Sigma(s_t), s_t | \kappa_\Sigma(s_t), p_{11}, p_{22}) \propto$$

$$\det(\Sigma(s_t))^{-\frac{K}{2}} \exp\left\{-\frac{1}{2} tr\left[\Sigma(s_t)^{-1}(Y - XA(s_t))'(Y - XA(s_t))\right]\right\}$$

$$\times \exp\left\{-\frac{1}{2} tr\left[\Sigma(s_t)^{-1}(A(s_t) - \underline{A}(s_t))'(\kappa_A(s_t)\underline{V}(s_t))^{-1}(A(s_t) - \underline{A}(s_t))\right]\right\}$$

$$\times \det(\Sigma(s_t))^{\frac{\nu+N+1}{2}} \exp\left\{-\frac{1}{2} tr\left[\Sigma(s_t)^{-1}\kappa_\Sigma(s_t)\right]\right\} \times p_{11}^{\bar{\tau_{11}}}(1-p_{11})^{\bar{\tau_{12}}} p_{22}^{\bar{\tau_{22}}}(1-p_{22})^{\bar{\tau_{21}}}$$

with parameters:

$$\bar{V(s_t)} = (X'(s_t)X(s_t) + (\kappa_A(s_t)\underline{V}(s_t)))^{-1}, \tag{2.41}$$

$$\bar{A(s_t)} = \bar{V(s_t)}(X(s_t)'Y(s_t) + (\kappa_A(s_t)\underline{V}(s_t)^{-1}\underline{A}(s_t))), \tag{2.42}$$

$$\bar{S}(s_t) = I_N\kappa_\sigma(s_t) + Y'(s_t)Y(s_t) + \underline{A}(s_t)'(\kappa_A(s_t)\underline{V}(s_t))^{-1}\underline{A}(s_t) - \bar{A}(s_t)'\bar{V(s_t)}^{-1}\bar{A}(s_t), \tag{2.43}$$

$$\bar{\nu} = T + \underline{\nu}, \tag{2.44}$$

$$\bar{\tau_{ij}} = \underline{\tau}_{ij} + n_{ij} \text{ for } i, j \in \{1, 2\}, \tag{2.45}$$

where n_{ij} specifies the number of one-step transitions from state i to j, following Chib (1996) notation. So, when it comes to our Matrix-Variate-Normal and Inverse-Wishart distributions, they closely resemble our hierarchical model. The main difference is that now we need to perform two separate simulations, each with its own unique prior settings. Additionally, we must calculate the transition probability and determine the regime for each specific t.

2.4.1 Posterior Distribution

Given the transition probability obtained from the Beta distribution posterior parameters, with a random initialization of n_{ij}, we can compute the smoothed states s_t, $t \in 1:T$ implementing the Hamiltonian Forward-Backward Filtering Algorithm in Hamilton (1989). Define $\upsilon = (A, \Sigma, \kappa_A, \kappa\_\Sigma, p_{11}, p_{22})$. In the forward step, calculate the one-step ahead prediction of s_t $p(s_t = 1|y^{t-1}, \upsilon) = p_{11}p(s_{t-1} = 1|y^{t-1}, \upsilon) + p_{21}p(s_{t-1} = 2|y^{t-1}, \upsilon)$ and similarly for $p(s_t = 2|y^{t-1}, \upsilon)$. Then filter for s_t through $p(s_t = 1|y^t, \upsilon) = \frac{p(y_t|s_t=1,y^{t-1,},\upsilon)p(s_t=1|y^{t-1},\upsilon)}{p(y_t|y^{t-1},\upsilon)}$, where $p(y_t|s_t = 1, y^{t-1,}, \upsilon)$ is obtained evaluating the parameters υ in the first regime at time $t-1$, and $p(y_t|y^{t-1}, \upsilon)$ is the summation of the numerator and its counterpart for the second state; repeat the filtering for all the times t in $\{1 \cdots T\}$. In the backward filter, for each $t = \{T-1, \cdots, 1\}$ the smoothed probability distribution is obtained through $p(s_t = 1|, y, \upsilon) = \sum_j^2 \frac{p_{1j}(t)p(s_t=1|y^t,\upsilon)p(s_{t+1}=j|y,\upsilon)}{\sum_i^2 p_{ij}(t)p(s_t=i|y^t,\upsilon)}$, where $p(s_T = j|y, \upsilon)$ is sampled from the multinomial sampler using the filtered probability at time T, and the other smoothed probabilities are obtained recursively.

2.4.2 Posterior Approximation

Initialize κ_A and κ_Σ at $\kappa_A^{(0)}$ and $\kappa_\Sigma^{(0)}$. Initialize the regimes for each time at random from a normal distribution. At each iteration i:

1. Draw $(A(s), \Sigma(s))^{(i)} \sim p(A(s), \Sigma(s) \| X(s), Y(s), \kappa_A(s)^{(i-1)}, \kappa_\Sigma(s)^{(i-1)}, s^{(i)}, p_{ij}^{(i)})$;
2. Draw $\kappa_A(s)^{(i)} \sim p(\kappa_A(s)|Y(s), X(s), \upsilon(s))$;
3. Draw $\kappa_\Sigma(s)^{(i)} \sim p(\kappa_\Sigma(s)|Y(s), X(s), \upsilon(s))$;

4. Draw $p_{ii}^{(i)} \sim p(p_{ii}|\upsilon(s), Y(s), X(s), s)$;

5. Draw $s_t^{(i)}$ from the multinomial distribution.

Repeat steps 1 and 2 for $(S_1 + S_2)$ times. Discard the first S_1 repetitions. Return the output as $\left\{A^{(i)}, \Sigma^{(i)}, \kappa_A^{(i)}, \kappa_\Sigma^{(i)}, p_{ii}^{(i)}, s_t^{(i)}\right\}_{i=S_1+1}^{S_2}$.

Chapter 3

Data Description

We download the data directly from the website of Miranda-Agrippino. The two authors study the consequences of a 1% increase in the U.S. monetary policy considering:

1. a domestic VAR with the effects on domestic financial markets and macroeconomic aggregates in the United States;
2. a global VAR with the effects on global asset markets, global domestic credit and international capital flows;
3. a "floaters" VAR to study if a fixed or pegged exchange rate affects the global contraction.

We will study the global specification, and include the variables in Figure 3.1, Figure 3.2, and Figure 3.3.

Against this framework, our interest is to study the degree by which U.S. monetary policy shocks can

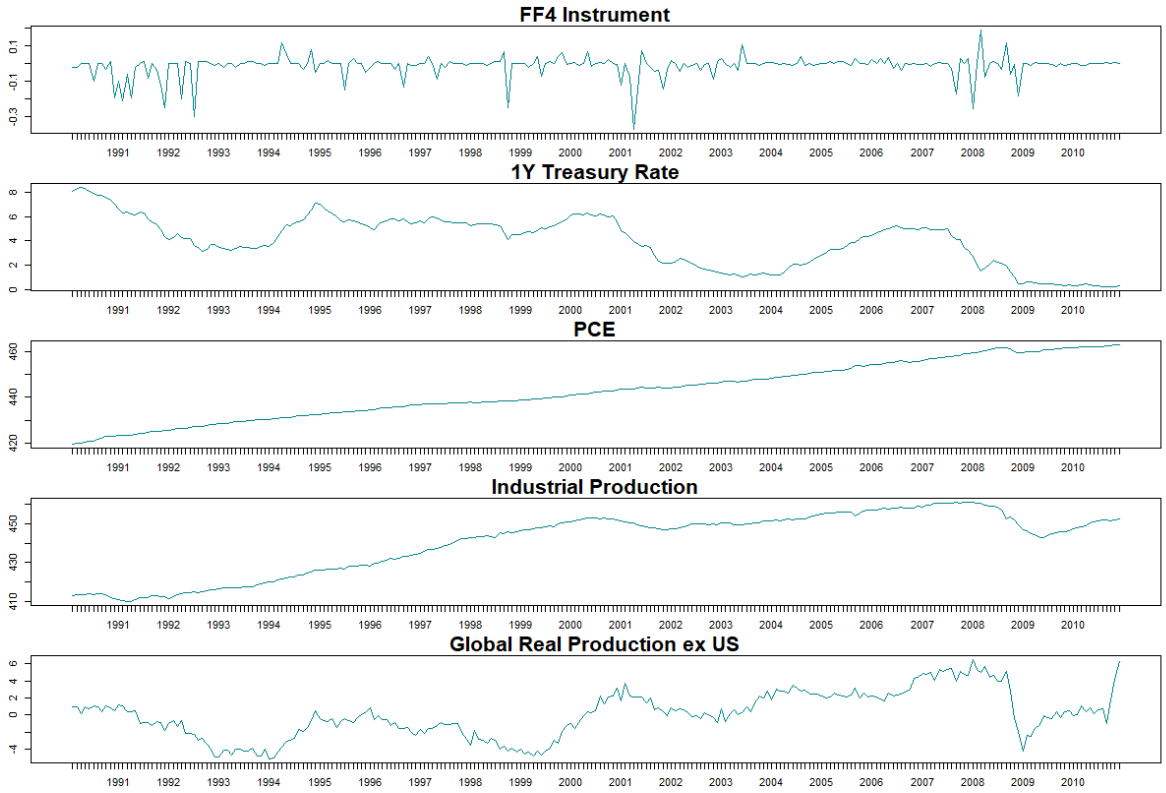

Figure 3.1: Time series plot of the endogenous variables at monthly frequencies for the 1990:1-2012:12 sample, including the Fourth Federal Fund Futures Contract (FF4) Instrument, the 1 Year Treasury Rate of the FED, the Personal Consumption Expenditures (PCE), Industrial Production of the U.S., and The Global Real Production excluding the U.S.

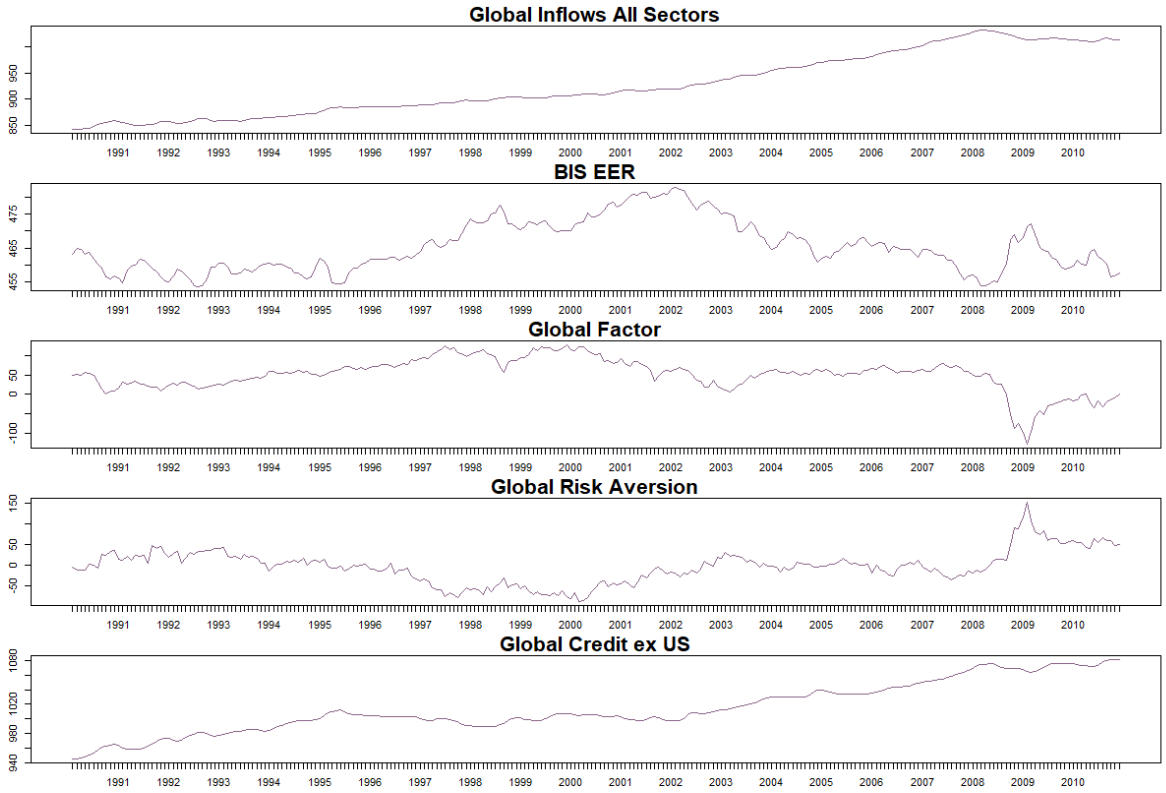

Figure 3.2: Time series plot of the endogenous variables at monthly frequencies for the 1990:1-2012:12 sample, including Global Inflows for all Sectors, the BIS Effective Exchange Rate (EER), the Miranda-Agrippino and Rey (2020) Global Factor and Global Risk Aversion, and Global Credit excluding the U.S.

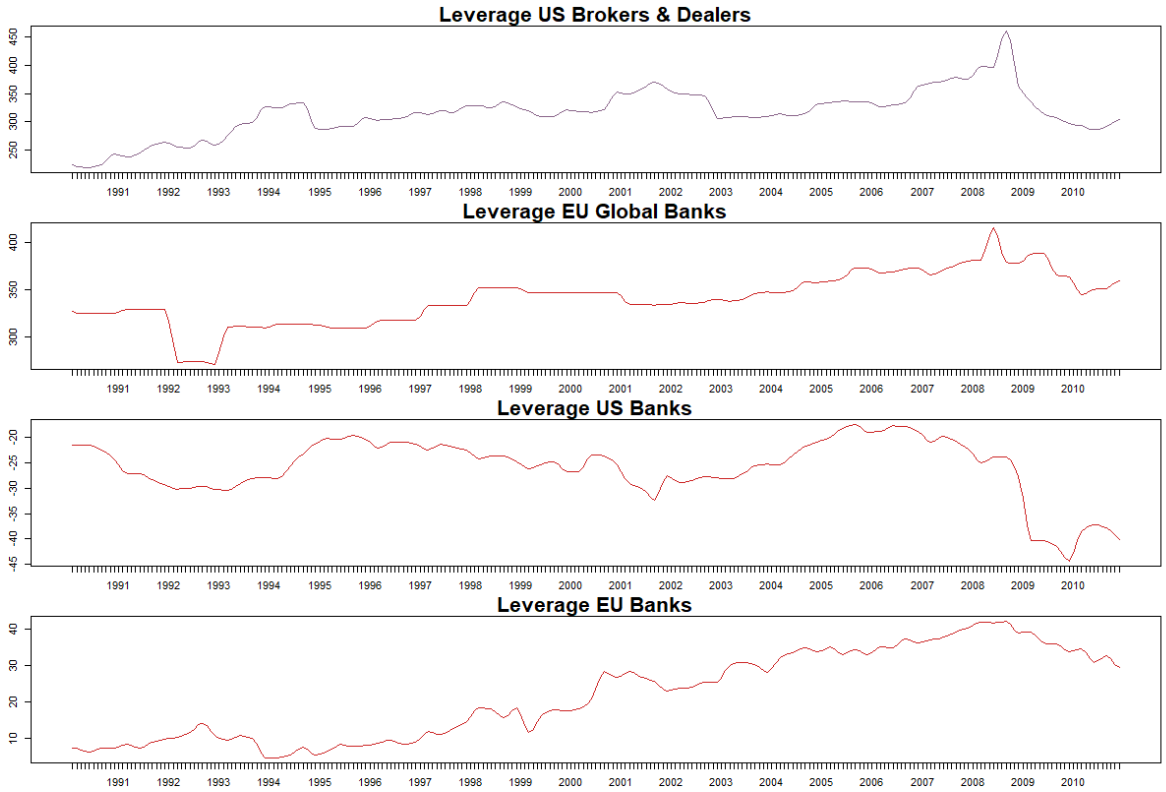

Figure 3.3: Time series plot of the endogenous variables at monthly frequencies for the 1990:1-2012:12 sample, including the leverage of US Brokers and Dealers, EU Global Banks, US Banks, and EU banks

propagate throughout the world's economies. In order to have a global picture we study macroeconomic variables that are affected and influenced by a FED change in the interest rate. The global variable included are constructed by scrutinizing the major global markets.[1]

We include the following variables:

1. the U.S. industrial production index that measures the real output of all relevant establishments located in the U.S.;
2. the Personal Consumption Expenditures (PCE) of the U.S.;
3. the Bank for International Settlement (BIS) effective exchange rate (EER) for the United States, i.e. a summary measure calculated by the BIS to account for changes in the U.S. bilateral exchange rate against other countries by their trade importance;
4. global inflows, defined as direct cross-border credit flows from the U.S. to the aforementioned countries' banks and non-bank recipients. This variable is pivotal to explain the degree of financial dependency of the rest of the world vis-à-vis the financial hegemon;
5. global domestic credit, another key variable in our VAR that outlines the total amount of funds in the world economy, including loans, debt instruments, and other forms of credit provided by financial institutions;
6. the FED policy rate coupled with the global real economic activity index (excluding the US). We can observe the lag effect of an increase in interest rates with a decrease in international

[1] Including Argentina, Australia, Austria, Belarus, Belgium, Bolivia, Brazil, Bulgaria, Canada, Chile, Colombia, Costa Rica, Croatia, Cyprus, Czech Republic, Denmark, Ecuador, Finland, France, Germany, Greece, Hong Kong, Hungary, Iceland, Indonesia, Ireland, Italy, Japan, Latvia, Lithuania, Luxembourg, Malaysia, Malta, Mexico, Netherlands, New Zealand, Norway, Poland, Portugal, Romania, Russia, Serbia, Singapore, Slovakia, Slovenia, South Africa, South Korea, Spain, Sweden, Switzerland, Thailand, Turkey, U.K., and the U.S.

economic activity;

7. the global factor discussed in the introductory chapter, rotated to provide an intuitive view that an increase in the factor reflects an increase in world asset prices.
8. global risk aversion, obtained as the inverse of the residual of the projection of the global factor on the monthly global realized variance measured using the MSCI index, a measure of performance of global stocks.

Then, we outline four types of leverage. First of all, leverage can be defined as the ratio between assets and equity, with equity being the difference between assets and debts. In finance, this measurement refers to the use of borrowed funds to finance assets or investments. Against this backdrop, the authors construct this variable as the ratio between claims in the private sector, i.e. credit extended by banks and other financial institutions to the private sector, and the sum of transferable deposits held by depository corporations, excluding central banks. This ratio reflects the proportion of credit extended to the private sector relative to deposits held by depository corporations, excluding central banks. A higher ratio suggests a higher banking leverage level. The authors differentiate between different leverages given financial agents' risk-taking behavior. As a matter of fact, we can observe that the leverage between EU global banks and US brokers and dealers is much larger than the leverage of big but not systemic EU and US banks. EU global banks include systematically important banks such as UBS and Unicredit. The importance of EU Global banks in influencing credit conditions in the U.S. has been documented by Shin (2012). Global banks' leverage is high for several reasons such as size and risk appetite. Brokers and dealers' behavior can be explained by their risk-loving approach.

Lastly, we will add the aforementioned instrument on top of the y_t variable. In the next section, we will provide the reason for this procedure.

3.1 Autocorrelation Analysis

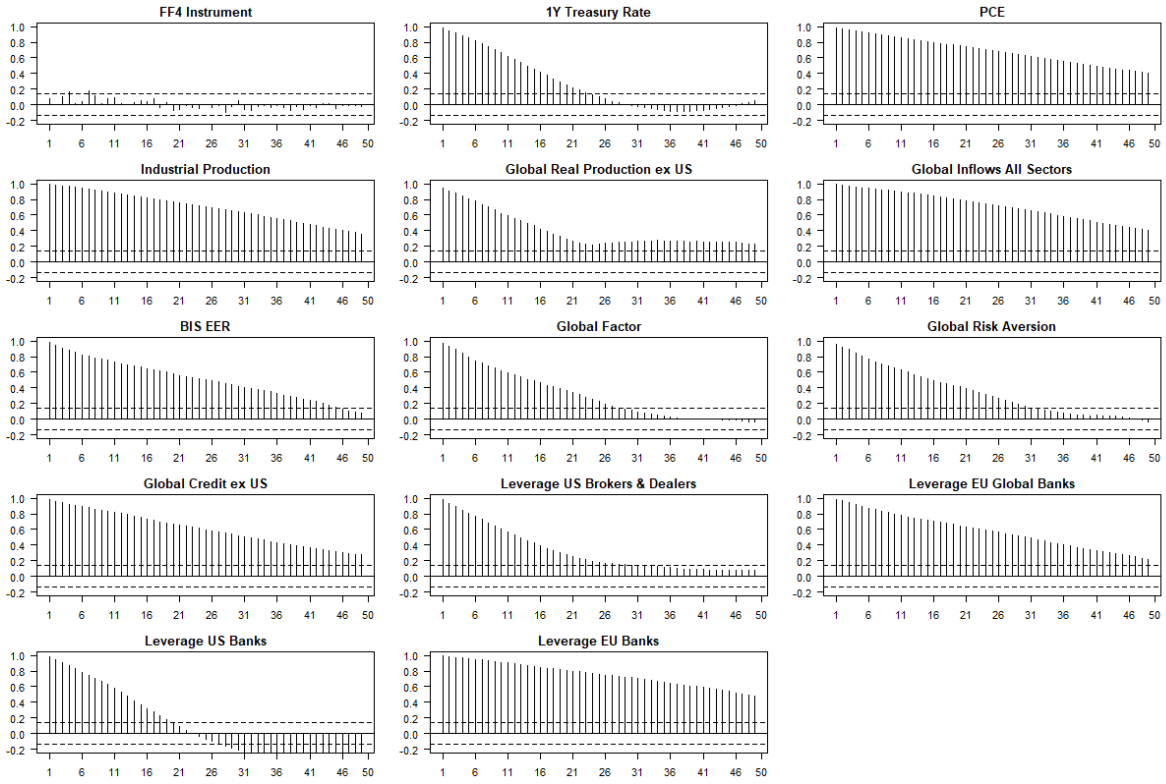

Figure 3.4: Autocorrelation Plots (ACF) at 50 lags of the variables in level terms

When we look at the autocorrelation plots (ACF) for our variables in Figure 3.4 at 50 lags, we observe a robust and positive autocorrelation pattern that slowly decreases over time, except for our instrument. Additionally, the partial autocorrelation plots (PACF) in Figure 3.5 reveal a nearly one value at the first lag and statistically insignificant values at later time lags. This suggests that these macroeconomic

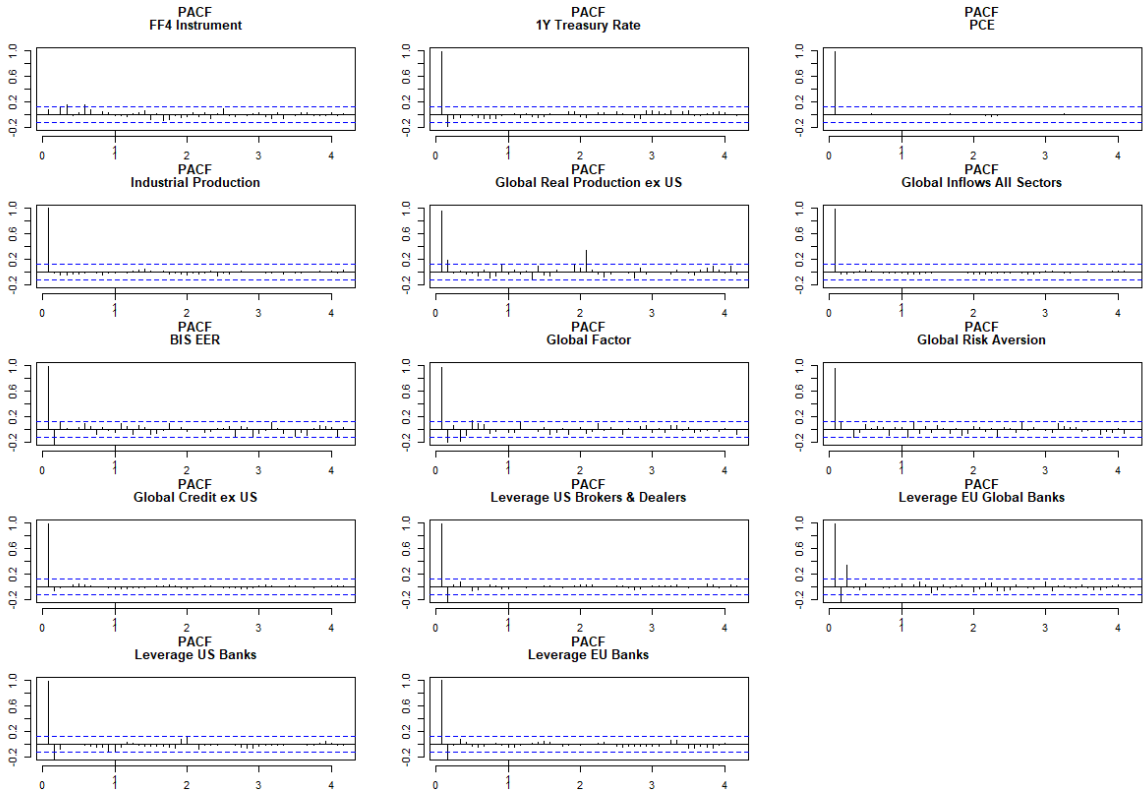

Figure 3.5: Partial Autocorrelation Plots (PACF) at 50 lags of the variables in level terms

variables behave like a random walk with a drift component and, as a result, are considered non-stationary due to the presence of a unit root. Hence, the dynamic models we have presented are an ideal candidate to handle the non-stationarities and non-linearities of the data.

Chapter 4

Empirical Results

Figure 4.1 reports the posterior mean of the first cell of three matrices: A, Σ, and B. This helps us get a sense of what these matrices look like under different specifications. In the context of our analysis, the autoregressive parameter A increases when we use the hierarchical prior structure, but it decreases when we switch to the Stochastic Volatility model. Similar patterns can be observed for Σ. On the other hand, in the Markov Switching (MS) model, we have fewer data points for each regime compared to the other specifications. As a result, our parameter estimates tend to show more variability. It is interesting to note that the Hierarchical model A is higher than the MS low volatility counterpart.

Furthermore, it is important to consider the values of the hyperprior parameters κ_A and κ_Σ as shown in Figure 4.2. We can see that the hyperprior parameter κ_A for the Hierarchical model has a very high value, which could potentially affect our results. This influence can be seen in the Impulse

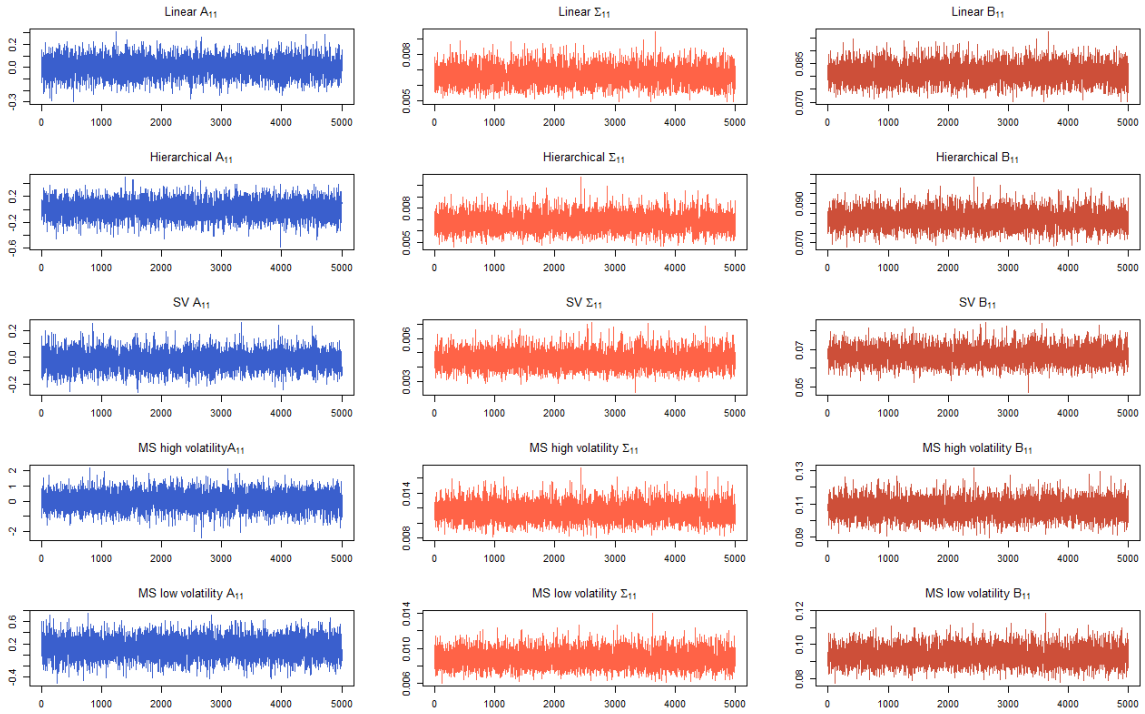

Figure 4.1: MCMC samples for 5000 draws with 10 thousands iterations of burn-in from the posterior probabilities of the first cell (the instrument variable) of the autoregressive parameter (in blue), the variance-covariance matrix (in orange), and the contemporaneous effects matrix (in red)

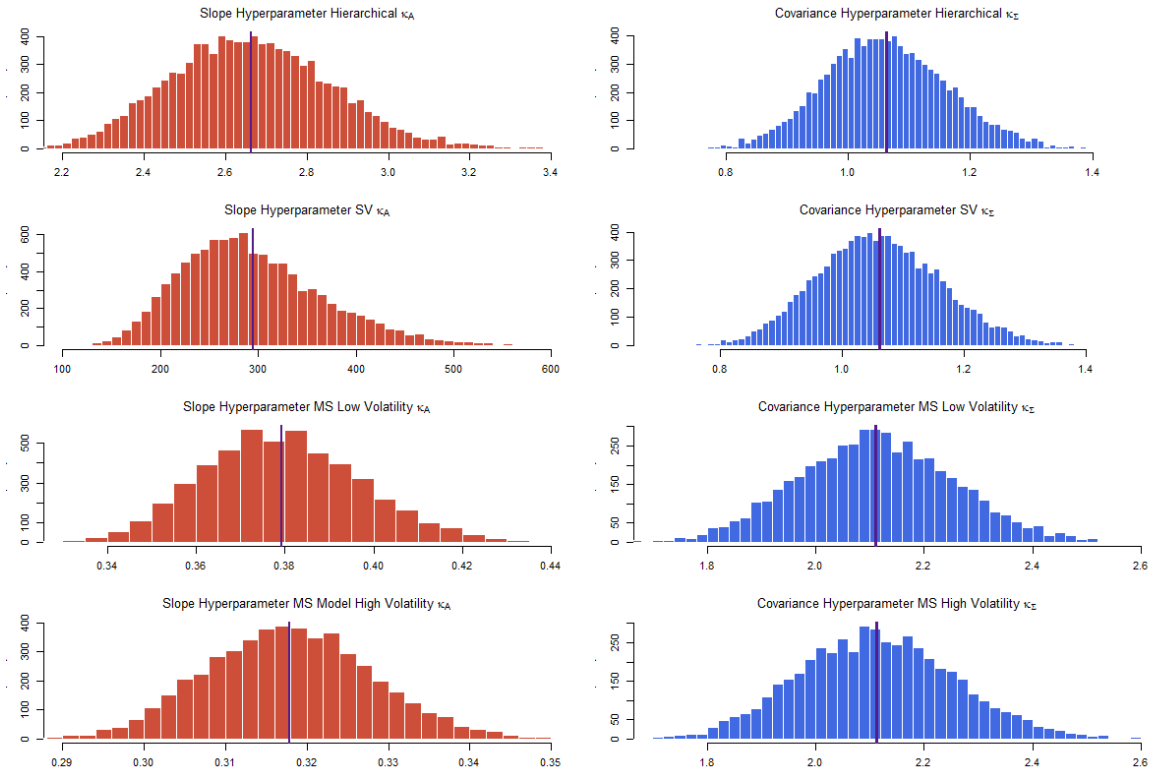

Figure 4.2: Histogram of the MCMC samples for 5000 draws with 10 thousands iterations of burn-in from the posterior probabilities of the hyperior parameters of the autoregressive coefficient (in red), and the variance-covariance matrix (in blue)

Response Functions (IRFs) presented in Figure 4.9. We have noticed that the posterior results of these κ parameters are strongly influenced by the parameters' initial values used in the Gamma and Inverse Gamma distributions approximations. In our future research, we plan to focus on improving the tuning of these hyperpriors to enhance the accuracy of our analysis.

4.0.1 Estimated Stochastic Volatility

Our algorithm in the Stochastic Volatility BVAR effectively estimates the volatility (represented by σ^2) during significant financial turbulence periods, such as the Japanese Asset Price Bubble in the early 1990s, the UK Black Wednesday, the Russian Financial Crisis of 1998, the Stock Market Downturn of 2002 following the Dot-Com Bubble burst, and, notably, the Global Financial Crisis that began in 2007-08. In Figure 4.3, we present a graphical representation of these estimates alongside Global Risk Aversion.

4.0.2 Markov Switching Results

We can observe that our Markov Switching model behaves as expected, with the states that follow closely the estimated volatility of the Stochastic Volatility model. The transition probability results show that there is high persistence of the second regime, i.e. the state with low volatility, whereas the other regime tends to be very volatile and with little persistence. Further draws would be needed to assess convergence, but due to our small computational power we can only draw 15 thousand iterations.

Moreover, we report the posterior distribution MCMC draws of the parameter of the Beta distribution

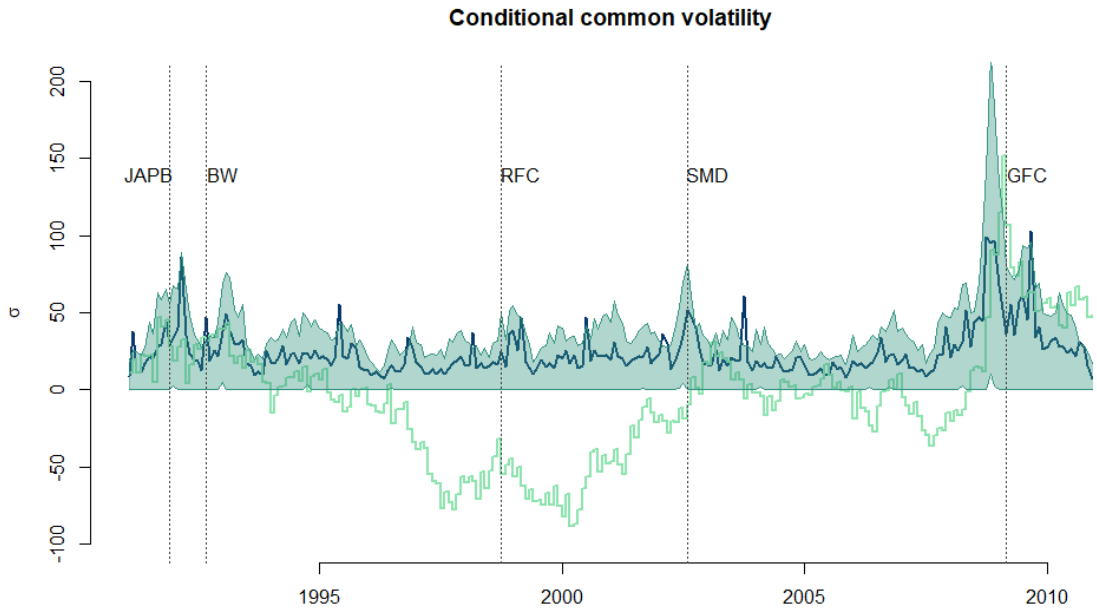

Figure 4.3: Estimated Stochastic Volatility Plot (in blue) with Global Risk Aversion (in green)

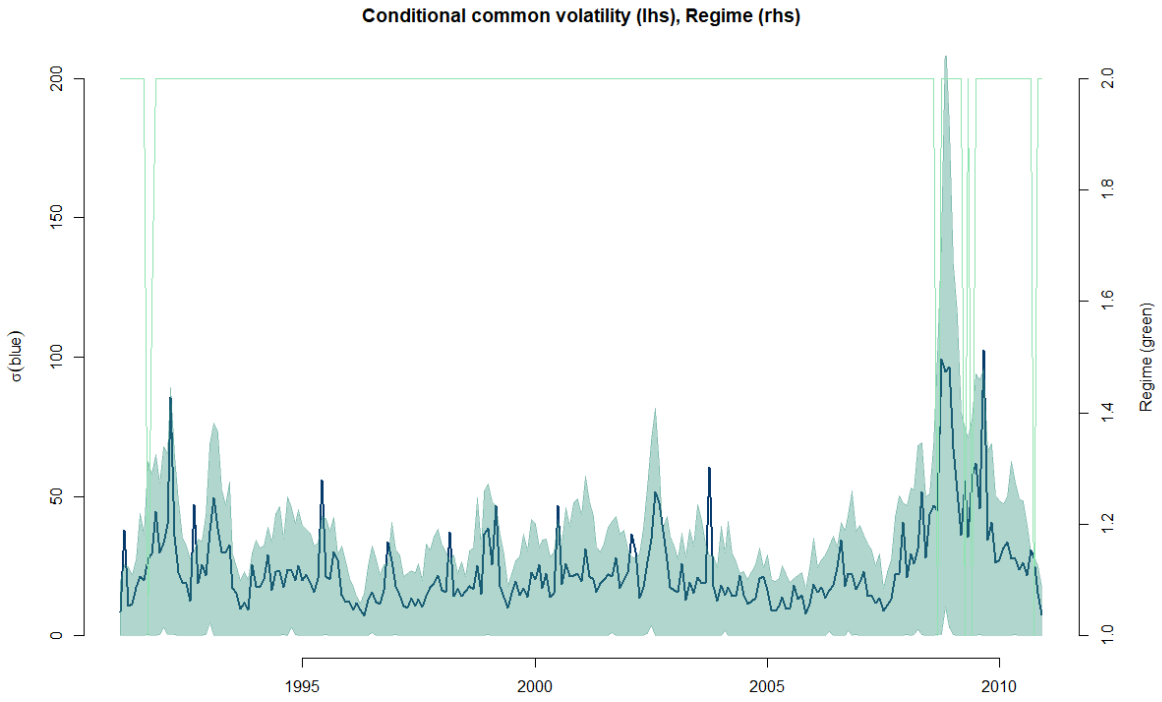

Figure 4.4: Markov Switching States (in green) and the estimated Stochastic Volatility (in blue)

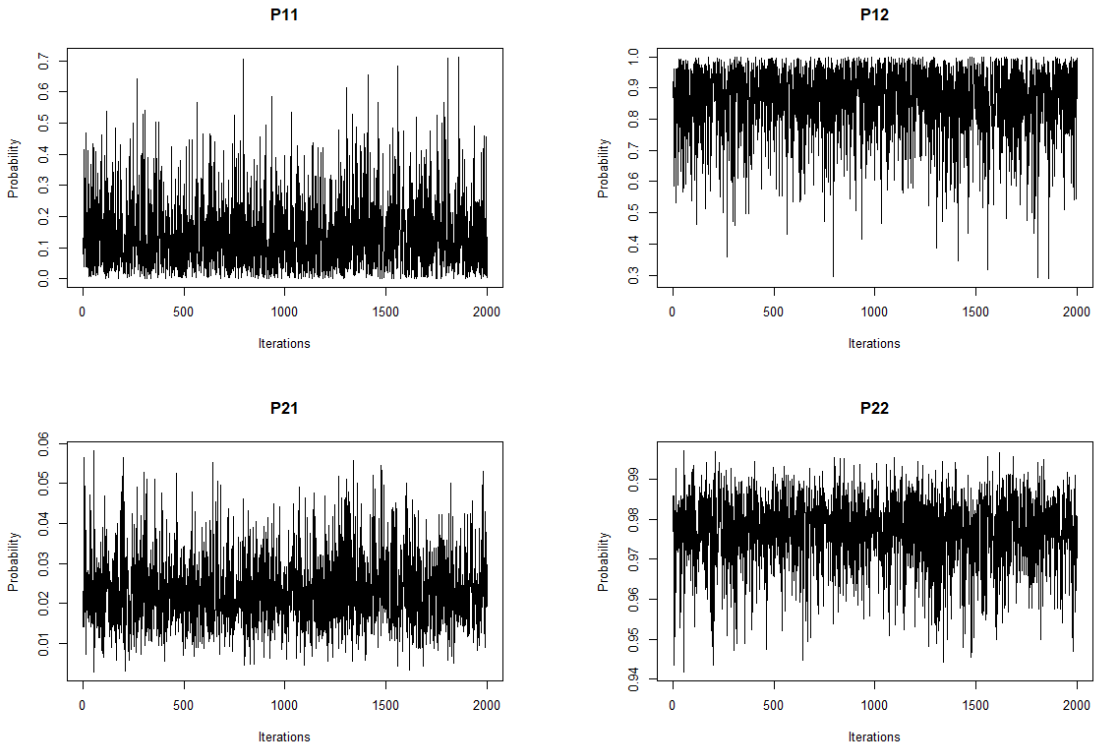

Figure 4.5: MCMC samples from the posterior probabilities of the transition probabilities

η_{ij} in Figure 4.6. We can observe that the parameters converge nicely, with the concentration of the regimes in the bottom right quadrant, which represents the number of occurrences of state 2 repeating itself.

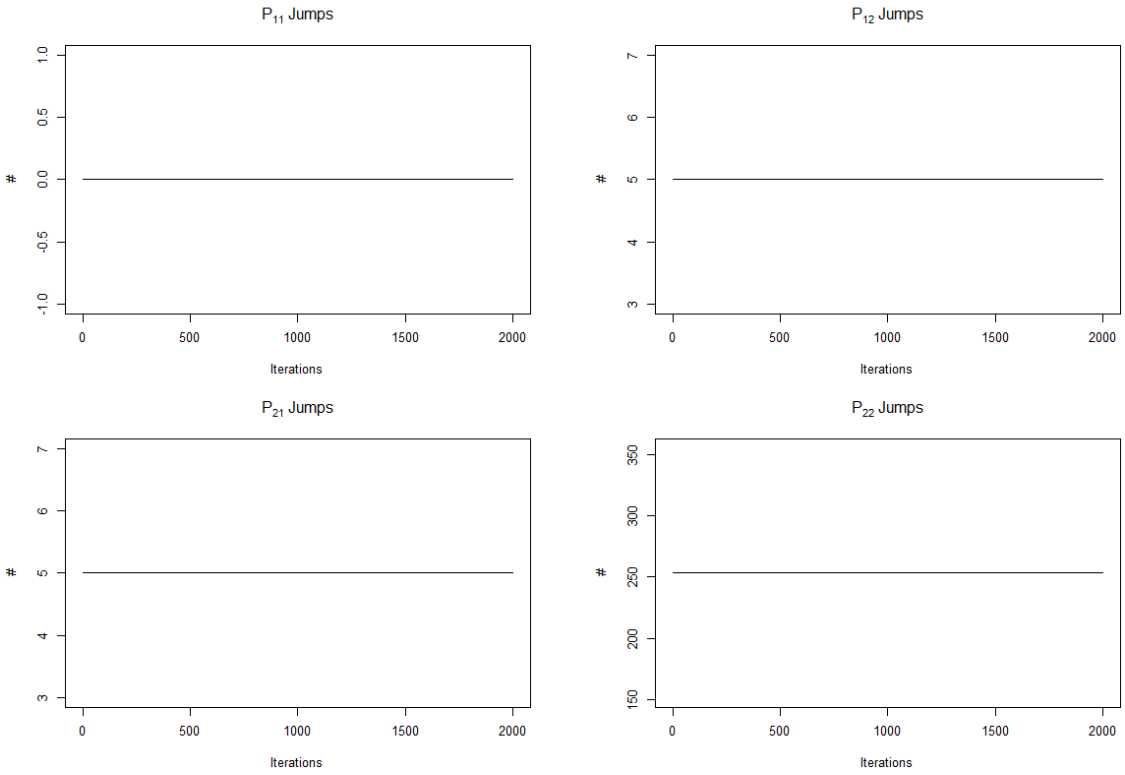

Figure 4.6: 2000 MCMC samples from the posterior probabilities of the Beta distribution parameters

4.1 Impulse Response Functions

The impulse response functions are the dynamic causal effects of the underlying shocks u_t on the economic measurements y_t (Kilian, Lütkepohl (2017)). Our model features the instrument in the first position. We will compute impulse response functions (IRFs) assuming that the instrument affects all

the other variables exogenously. We define an IRF as a shock of the first variable in u_t (the instrument) on the 14 variables n of our model in Y_t at time t until time $t+i$. In our case $i = 24$ because we want to study the IRFs for two years as the original paper authors do. Compactly, we can describe the computations as follows:

$$\frac{\partial y_{n.t+1}}{\partial u_{1.t}} = \theta_{nj.1}. \tag{4.1}$$

The assumption of Plagborg-Moller and Wolf (2021) regarding the invertibility of ε is satisfied given a Cholesky Decomposition. From our IRFs, we compute Forecast Error Variance Decompositions (FEVD):

$\mathbb{V}ar\left[u_{t+h|t}\right] = \Xi\left[\left(y_{t+h} - y_{t+h|t}\right)\left(y_{t+h} - y_{t+h|t}\right)'\right] =$

$\Xi\left[\left(\Phi_0 u_{t+h} + \cdots + \Phi_{h-1}u_{t+1}\right)\left(\Phi_0 u_{t+h} + \cdots + \Phi_{h-1}u_{t+1}\right)'\right] =$

$\Xi\left[\left(\Theta_0 \epsilon_{t+h} + \cdots + \Theta_{h-1}\epsilon_{t+1}\right)\left(\Theta_0 \epsilon_{t+h} + \cdots + \Theta_{h-1}\epsilon_{t+1}\right)'\right] =$

$\Theta_0 \Xi\left[\Xi_{t+1}\left[\epsilon_{t+h}\epsilon'_{t+h}\right]\Theta'_0\right] + \cdots + \Theta_{h-1}\Xi\left[\Xi_t\left[\epsilon_{t+1}\epsilon'_{t+1}\right]\Theta'_0\right] =$

$\Theta_0\Theta'_0 + \cdots + \Theta_{h-1}\Theta'_{h-1}.$

4.1.1 IRFs Basic Model

We will outline IRFs for both our basic and extended models, computing 10 thousand draws for our estimates. For our empirical estimation we employ a SVAR(12) as Miranda-Agrippino and Rey (2020), and we normalize the IRFs so that the Treasury rate has a percentage point increase at horizon 0. From the 14 variables, we present only 10 of them. We abstain from plotting the global factor because

it provides inverted results of global risk aversion. In addition, we do not plot US brokers & dealers' leverage and US banks' leverage. This is because our main interests lie in spillovers of monetary policy outside the US. The abscissa scale is in months, given that we use monthly variables, and display the 68% and 90% density intervals. We will briefly outline the results. Upon realisation, the one-year Treasury rate spikes in the first quarter, then it decreases and increases in the third and fourth quarter, hoovering around zero in the remaining lags; we observe the PCE deflator to shrink in the first three quarters and increases thereafter; industrial production shrinks in the first three quarters, and then mean-reverts; global real production excluding the financial hegemon provides insignificant results in the first two lags and then increases, similarly to global inflows; the BIS real effective exchange rate increases upon realisation as expected following the monetary policy shock, decreasing from the second quarter onwards; global risk aversion - the proxy for global risky asset prices - spikes and hoovers around zero from the third quarter; global credit excluding the US decreases as expected in the first two quarters and then increases thereafter; the leverage drop immediately, but contrary to the original paper it does not mean-revert in the first quarter, and EU banks' leverage provides insignificant results;

4.1.2 FEVD Basic Model

Moreover, we include FEVD of two variables, i.e. EU Global banks' leverage, and EU big but not systemic banks' leverage. FEVD provide the information of how much each variable contributes to the information of the other variables' forecast variability at each horizon. We can observe that the FEVD

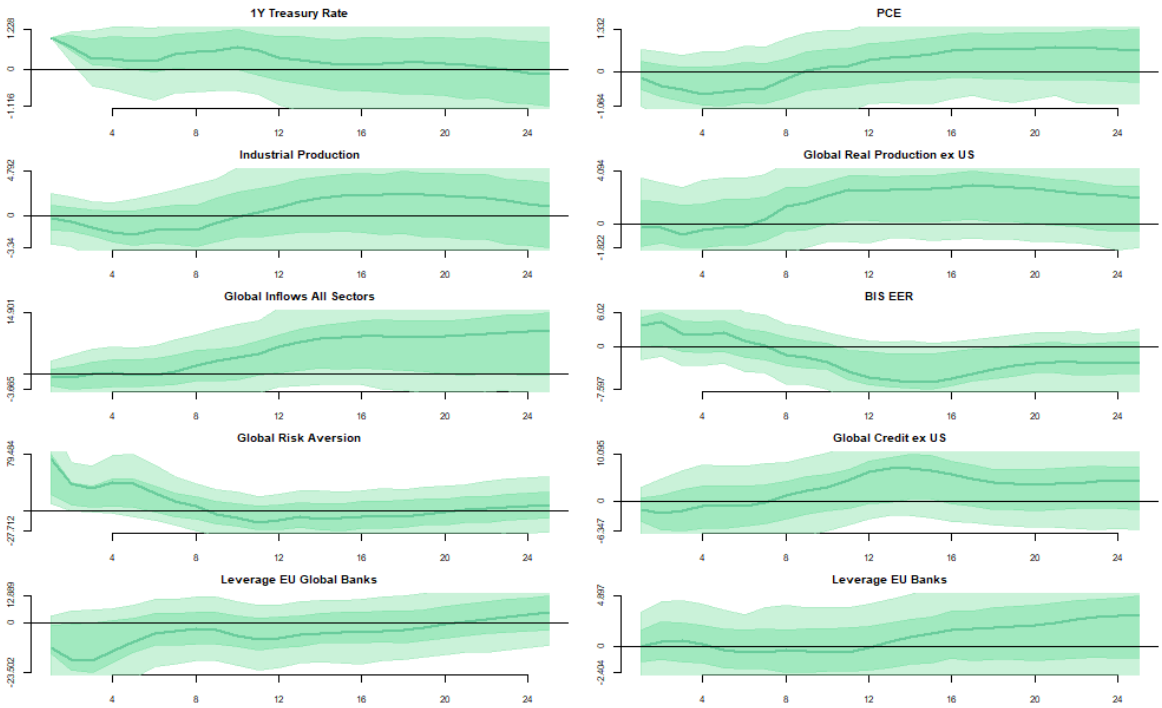

Figure 4.7: Impulse Response Functions (IRFs) Plot of the Linear Bayesian SVAR Model

for Global banks and the other variables account significantly for the aforementioned information at further horizons. The larger contributors at the last horizon are the leverage of US and EU global but not systematically important banks (>38%). In addition, similar conclusions can be drawn to the FEVD of EU big but systematic banks' leverage. Other larger contributors at the last horizon are Leverage for EU global banks and US banks. FEVD for the other models look similar and therefore are only reported in the appendix.

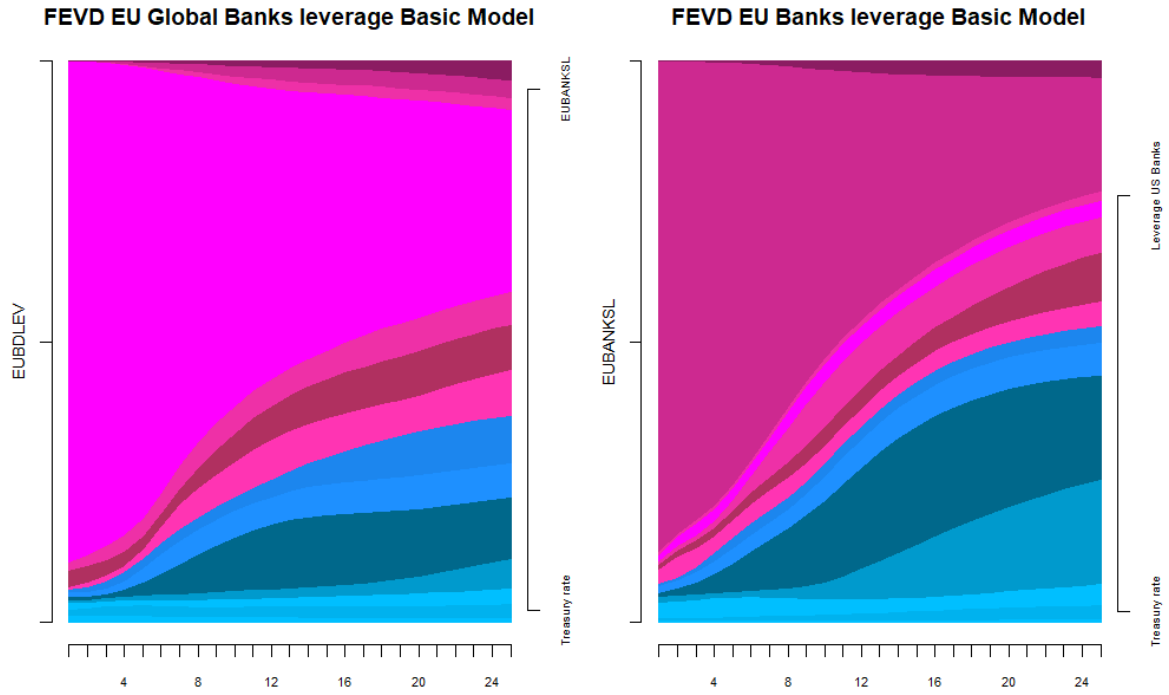

Figure 4.8: Forecast Error Variance Decomposition (FEVD) Plot of the Linear Bayesian SVAR Model for the Leverage of EU Global Banks and EU Banks

4.1.3 IRFs Extended Model

Regarding the extended model, the IRFs are generally in line with previous results or expectations. Generally, we observe significant responses to be temporary and not persistent. The treasury rate decreases upon realization of the shock and then hovers around zero. The PCE displays a puzzling behavior, increasing in the all quarters following the shock. The remaining variables show a similar pattern compared to the basic model, but in general, we can observe less insightful shapes, maybe due to hyperprior sensitivity of our results. We have worked on tuning different parameters for the κ_A and κ_Σ, but we still have to improve our prior selection. This will be done in future work.

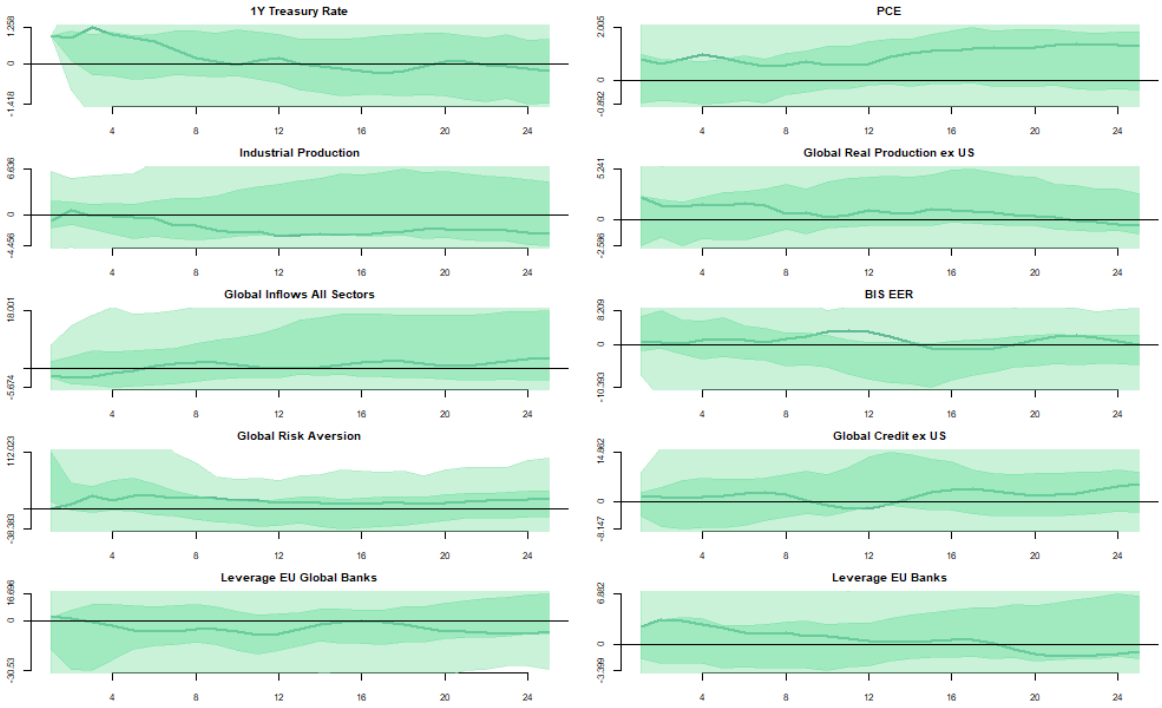

Figure 4.9: Impulse Response Functions (IRFs) of the Hierarchical Model

4.1.4 IRFs SV Model

Plots of IRFs for the Stochastic Volatility provide little insight, they are not smooth and have erratic movements around zero. Further work is needed to improve these results.

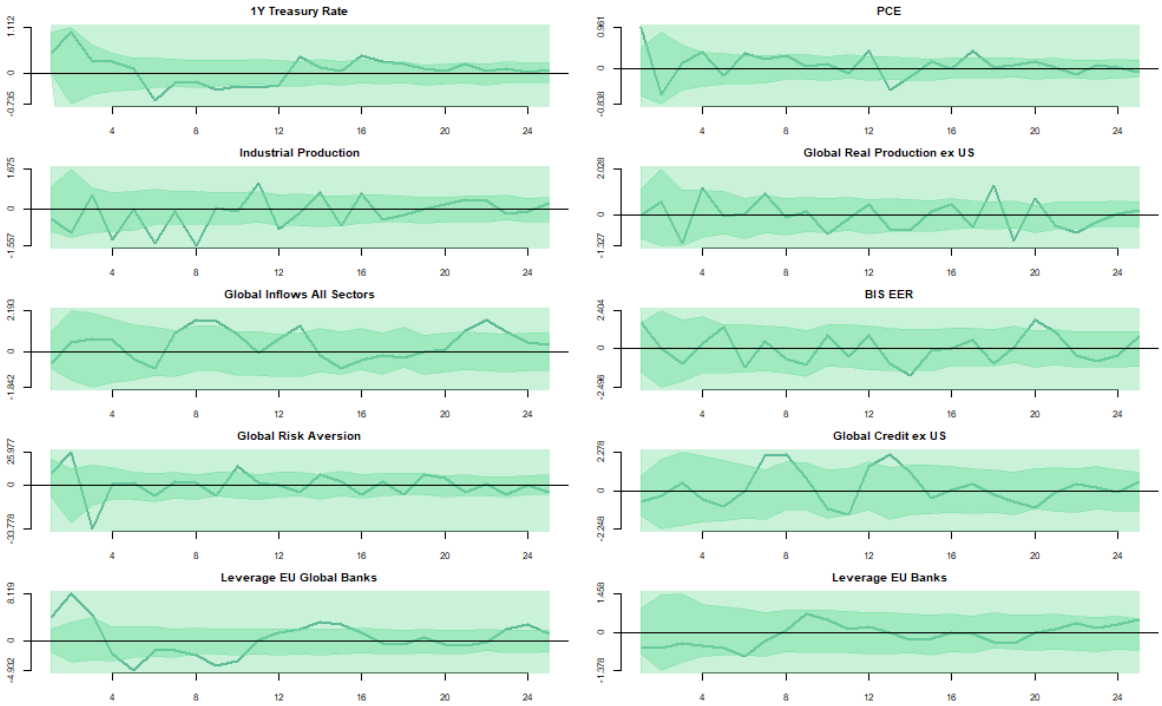

Figure 4.10: Impulse Response Functions (IRFs) Plot of the Stochastic Volatility Model

4.1.5 IRFs Markov Switching Model

For our MS model we propose three IRFs. Two of these are given from the distinct full conditional posterior distributions of our parameters for the different regimes. A third IRF is provided as a weighted IRF between the two states, where we forecast the two future regimes' weights given the IRF

computed in the future. Hence, this particular IRF in our MS framework is given as

$$\Xi(\Xi(Y_{T+1}|\upsilon_T, s_{T+1})|\upsilon_T) = \sum_{j=1}^{2} p(s_{T+1}|\upsilon_T) IRF(s_{T+1} = j), \tag{4.2}$$

where the inner expectation is equal to $IRF(s_{T+1})$ and

$$p(s_{T+1}|\upsilon_T) = \sum_{i=1}^{2} p(s_{T+1} = j|s_T = i) p(s_T|\upsilon_T) \tag{4.3}$$

where the first term can be obtained from our Gibbs Sampler and the second term is estimated from the Hamiltonian Forward-Backward Algorithm. We can observe that in periods of High volatility a shock to the treasury rate is associated with an insignificant response in all the variables. This may be due to the small number of data points used to estimate these shocks. On the other hand, the weighted IRFs follow closely the Low Volatility IRFs. The results of these IRFs generally provide insignificant results, but there are nice exceptions on the first quarters like for the leverage of the EU Global Banks, Global Risk Aversion, Global Credit, and the BIS EER.

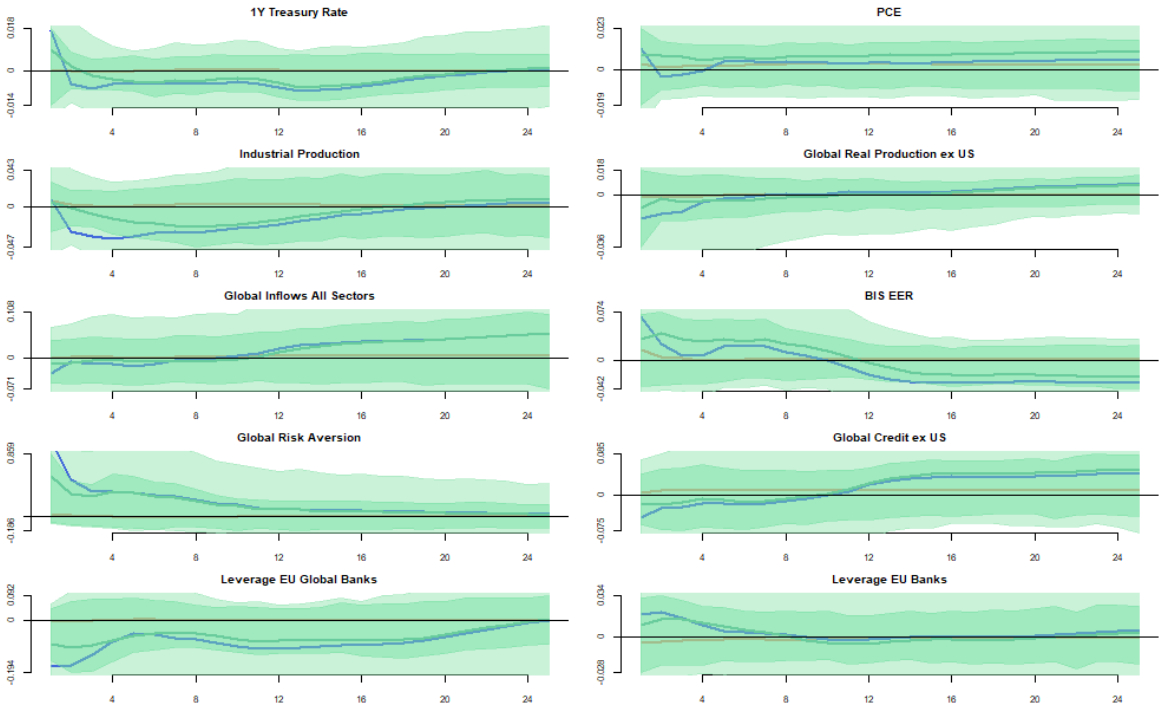

Figure 4.11: IRF Plot of the Markov-Switching Model - Weighted IRF (green); IRF high volatility (red); IRF low volatility (blue)

Chapter 5

Conclusion

In our project, we have used four different methods to estimate a Bayesian Structural Vector Autoregression (SVAR) model, implementing the framework of Miranda-Agrippino and Rey (2020). We have dealt with hierarchical modelling, with two additional extensions implementing Stochastic Volatility and Markov-Switching. We have derived the posterior distributions and we have approximated their results via Gibbs Sampling. In the hierarchical model we have seen that the tuning of the hyper-prior parameters is a fundamental driver for the posterior distribution approximations, and we need to improve the tuning of the κs to gain more insights from our results. The priors are particularly important in our model because we implement a VAR with 12 lags and 14 variables, and given only 251 data points it is of paramount importance to have a good prior specification. With regard to the Stochastic Volatility model, we have estimated nicely the time varying volatility of our dataset,

that captures the main financial busts of our time series span. Lastly, in the Markov-Switching model identified through periods of high and low volatility, the regimes follow the aforementioned stochastic volatility, and the transition probability displays persistency in the low-volatility state as expected. In the Impulse Response Functions (IRFs), we observe the most plausible responses using a linear model without hyperprior parameters. It may be that simple models can offer strong explanations. Nevertheless, there is more work ahead to ensure our results are consistently smooth, as pointed out in the study by Miranda-Agrippino and Rey (2020). In particular, the IRFs for the remaining models do not seem to provide realistic results. Furthermore, we have not quantified the model fits, and the next step will include the computation of marginal likelihood, for instance using Chib (1996). Despite the challenges, going through the process of developing and coding these models has been a valuable exercise. It is important to note that this work is not the final destination but rather a foundation for future research and improvements in our understanding of Bayesian Analysis.

References

Bańbura, Marta, Giannone Domenico, and Lucrezia Reichlin. 2010. "Large Bayesian Vector Auto Regressions." *Journal of Applied Econometrics* 25 (1): 71–92.

Baumeister, Christiane, and James D. Hamilton. 2006. "Structural Interpretation of Vector Autoregressions with Incomplete Identification: Revisiting the Role of Oil Supply and Demand Shocks." *American Economic Review* 109 (5): 1873–1910.

Bianchi, Daniele, Billio Monica, Casarin Roberto, and Massimo Guidolin. 2019. "Modeling Systemic Risk with Markov Switching Graphical SUR Models." *Journal of Econometrics* 210 (1): 58–74.

Billio, Monica, Casarin Roberto, Ravazzolo Francesco, and Herman K. Van Dijk. 2016. "Interconnections Between Eurozone and US Booms and Busts Using a Bayesian Panel Markov-Switching VAR Model." *Journal of Applied Econometrics* 31 (7): 1352–70.

Canova, Fabio, and Matteo Ciccarelli. 2009. "Estimating Multicountry VAR Models." *International Economic Review* 50 (3): 929–59.

Canova, Fabio, and Luca Gambetti. 2006. "Structural Changes in the US Economy: Bad Luck or Bad

Policy?" *CEPR Discussion Paper* 5457.

Carriero, Andrea, and E. Clark Todd. 2016. "Common Drifting Volatility in Large Bayesian VARs." *Review of Economics and Statistics* 81 (42): 608–16.

Casarin, Roberto, Sartore Domenico, and Marco Tronzano. 2017. "A Bayesian Markov-Switching Correlation Model for Contagion Analysis on Exchange Rate Markets." *Journal of Business & Economic Statistics* 36 (1): 101–14.

Chan, Joshua C.C, and Ivan Jeliazkov. 2009. "Joint Estimation of Model Parameters and Outlier Effects in Time Series." *International Journal of Mathematical Modelling and Numerical Optimisation* 1 (1-2): 284–97.

Chen, Chung, and Lon-Mu Liu. 1993. "Joint Estimation of Model Parameters and Outlier Effects in Time Series." *Journal of the American Statistical Association* 88 (421): 284–97.

Chib, Siddhartha. 1996. "Calculating Posterior Distributions and Modal Estimates in Markov Mixture Models." *Journal of Econometrics* 75: 76–97.

Christiano, Lawrence J., Eichenbaum Martin, and Charles Evans. 1996. "The Effects of Monetary Policy Shocks: Evidence from the Flow of Funds." *The Review of Economics and Statistics* 78 (1): 16–34.

Ciccarelli, Matteo, and Juan Angel García. 2021. "Expectation Spillovers and the Return of Inflation." *Economic Letters* 209 (110119.).

Clark, Todd E, and Francesco Ravazzolo. 2014. "Macroeconomic Forecasting Performance Under Alternative Specifications of Time-Varying Volatility." *Journal of Applied Econometrics* 30 (4):

551–75.

Cogley, Timothy, and Thomas J. Sargent. 2005. "Drifts and Volatilities: Monetary Policies and Outcomes in the Post WWII US." *Review of Economic Dynamics* 8: 262–302.

D'Agostino, Antonello, Gambetti Luca, and Domenico Giannone. 2013. "Macroeconomic Forecasting and Structural Change." *Journal of Applied Econometrics* 28 (1): 82–101.

Del Negro, Marco, and Frank Schorfheide. 2004. "Priors from General Equilibrium Models for Vars." *International Economic Review* 45 (2): 643–73.

Doan, Thomas, Sims Christopher A., and Robert B. Litterman. 1984. "Forecasting and Conditional Projection Using Realistic Prior Distribution." *Econometric Review* 3: 1–100.

Droumaguet, Matthieu, Warne Anders, and Tomasz Woźniak. 2017. "Granger Causality and Regime Inference in Markov Switching VAR Models with Bayesian Methods." *Journal of Applied Econometrics* 32 (4): 802–18.

Frühwirth-Schnatter, Sylvia. 2006. *Finite Mixture and Markov Switching Models*. Springer Science & Business Media.

Gertler, Mark, and Peter Karadi. 2015. "Monetary Policy Surprises, Credit Costs, and Economic Activity." *American Economic Journal: Macroeconomics* 7 (1): 44–76.

Giannone, Domenico, Michele Lenza, and Giorgio E. Primiceri. 2015. "Prior Selection for Vector Autoregressions." *The Review of Economics and Statistics* 97 (2): 436–51.

Gürkaynak, Refet S., Sack Brian, and Eric T. Swanson. 2005. "Do Actions Speak Louder Than Words? The Response of Asset Prices to Monetary Policy Actions and Statements." *International Journal*

of Central Banking 1: 55–93.

Hamilton, James D. 1989. "A New Approach to the Economic Analysis of Nonstationary Time Series and the Business Cycle." *Econometrica* 57 (2): 357–84.

———. 1994. *Time Series Analysis*. Princeton, NJ: Princeton University Press.

Herwartz, Helmut, Rohloff Hannes, and Shu Wang. 2021. "Proxy SVAR Identification of Monetary Policy Shocks - Monte Carlo Evidence and Insights for the US." *Journal of Economic Dynamics & Control* 139 (104457).

Jacquier, Eric, Polson Nicholas G, and Peter E. Rossi. 1994. "Bayesian Analysis of Stochastic Volatility Models." *Journal of Business & Economic Statistics* 12 (4): 371–89.

———. 2004. "Bayesian Analysis of Stochastic Volatility Models with Fat-Tails and Correlated Errors." *Journal of Econometrics* 122 (1): 185–212.

Karlsson, Sune. 2013. "Chapter 15 - Forecasting with Bayesian Vector Autoregression." *Handbook of Economic Forecasting* 2 (B): 781–97.

Kim, Chang-Jin, and Charles R. Nelson. 1998. "Business Cycle Turning Points, a New Coincident Index, and Tests of Duration Dependence Based on a Dynamic Factor Model with Regime Switching." *The Review of Economics and Statistics* 80 (2): 188–201.

———. 1999. "Has the US Economy Become More Stable? A Bayesian Approach Based on a Markov-Switching Model of the Business Cycle." *Review of Economics and Statistics* 81 (42): 608–16.

Koop, Gary, and Dimitris Korobilis. 2010. "Bayesian Multivariate Time Series Methods for Empirical Macroeconomics." *Foundations and Trends in Econometrics* 3 (4): 267–358.

Litterman, Robert. 1980. "A Bayesian Procedure for Forecasting with Vector Autoregression." *Working Paper, Massachusetts Institute of Technology, Dept. Of Economics*.

———. 2020. "Forecasting with Bayesian Vector Autoregressions-Five Years of Experience." *Journal of Business & Economic Statistics* 4 (1): 25–38.

Lütkepohl, Helmut, and Tomasz Woźniak. 2017. "Bayesian Inference for Structural Vector Autoregressions Identified by Markov-Switching Heteroskedasticity." *Journal of Economic Dynamics and Control* 113: 103862.

Mertens, Karel, and Morten O. Ravn. 2013. "The Dynamic Effects of Personal and Corporate Income Tax Changes in the United States." *American Economic Review* 103 (4): 1212–47.

Miranda-Agrippino, Silvia, and H'elene Rey. 2020. "US Monetary Policy and the Global Financial Cycle." *The Review of Economic Studies* 87 (6): 2754–76.

Omori, Yasuhiro, Siddhartha Chib, Neil Shephard, and Jouchi Nakajima. 2007. "Stochastic Volatility with Leverage: Fast and Efficient Likelihood Inference." *Journal of Econometrics* 140 (2): 425–49.

Plagborg-Moller, Mikkel, and Christian K. Wolf. 2021. "Local Projections and VARS Estimate the Same Impulse Reponses." *Econometrica* 89 (2): 955–80.

Primiceri, Giorgio E. 2005. "Time Varying Structural Vector Autoregressions and Monetary Policy." *The Review of Economic Studies* 72 (3): 821–52.

Shin, H. S. 2012. "Global Banking Glut and Loan Risk Premium." *IMF Economic Review* 60: 155–92.

Sims, Christopher A. 1980. "Macroeconomics and Reality." *Econometrics* 48 (1): 1–48.

Sims Christopher A., Waggoner Daniel, and Tao Zha. 2008. "Methods for Inference in Large Multiple-

Equation Markov-Switching Models." *Journal of Econometrics* 146 (2): 255–74.

Sims, Christopher A., and Tao Zha. 1998. "Bayesian Methods for Dynamic Multivariate Models." *International Economic Review* 39 (4): 949–68.

———. 2006. "Were There Regime Switches in US Monetary Policy?" *American Economic Review* 96 (1): 54–81.

Song, Yong, and Tomasz Woźniak. 2021. *Markov Switching*. Oxford Research Encyclopedias, Economics; Finance.

Woźniak, Tomasz. 2016. "Bayesian Vector Autoregressions." *Australian Economic Review* 49 (3): 365–80.

Appendix

Table 1: Augmented-Dickey-Fuller (ADF) Test on Level Variables {.striped .hover}

Variable Names	Dickey-Fuller	Lag	p-value	Dickey-Fuller diff	Lag diff	p-value diff
FF4 Instrument	-4.492	6	0.010	-10.666	6	0.01
1Y Treasury Rate	-2.612	6	0.318	-4.047	6	0.01
PCE	-2.349	6	0.429	-6.200	6	0.01
Industrial Production	-1.692	6	0.706	-4.354	6	0.01
Global Real Production ex US	-3.305	6	0.071	-5.053	6	0.01

Variable Names	Dickey-Fuller	Lag	p-value	Dickey-Fuller diff	Lag diff	p-value diff
Global Inflows All Sectors	-2.032	6	0.562	-4.474	6	0.01
BIS EER	-1.425	6	0.818	-7.129	6	0.01
Global Factor	-2.031	6	0.563	-7.166	6	0.01
Global Risk Aversion	-1.857	6	0.636	-6.564	6	0.01
Global Credit ex US	-1.520	6	0.778	-5.558	6	0.01
Leverage US Brokers & Dealers	-2.699	6	0.282	-5.411	6	0.01
Leverage EU Global Banks	-3.276	6	0.076	-5.696	6	0.01
Leverage US Banks	-1.529	6	0.774	-5.348	6	0.01
Leverage EU Banks	-1.637	6	0.729	-6.037	6	0.01

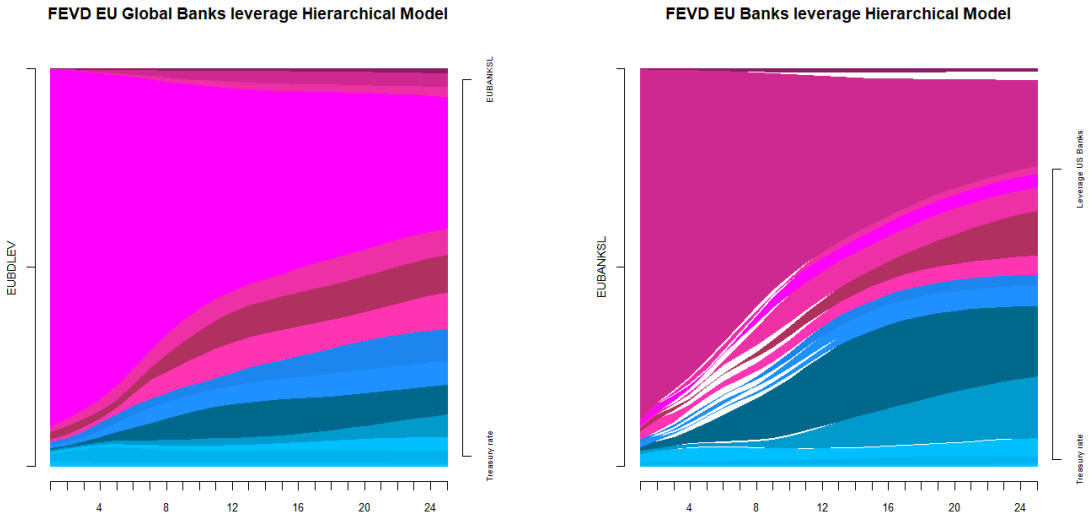

Figure 1: Forecast Error Variance Decomposition (FEVD) Plot of the Hierarchical Bayesian SVAR Model for the Leverage of EU Global Banks and EU Banks

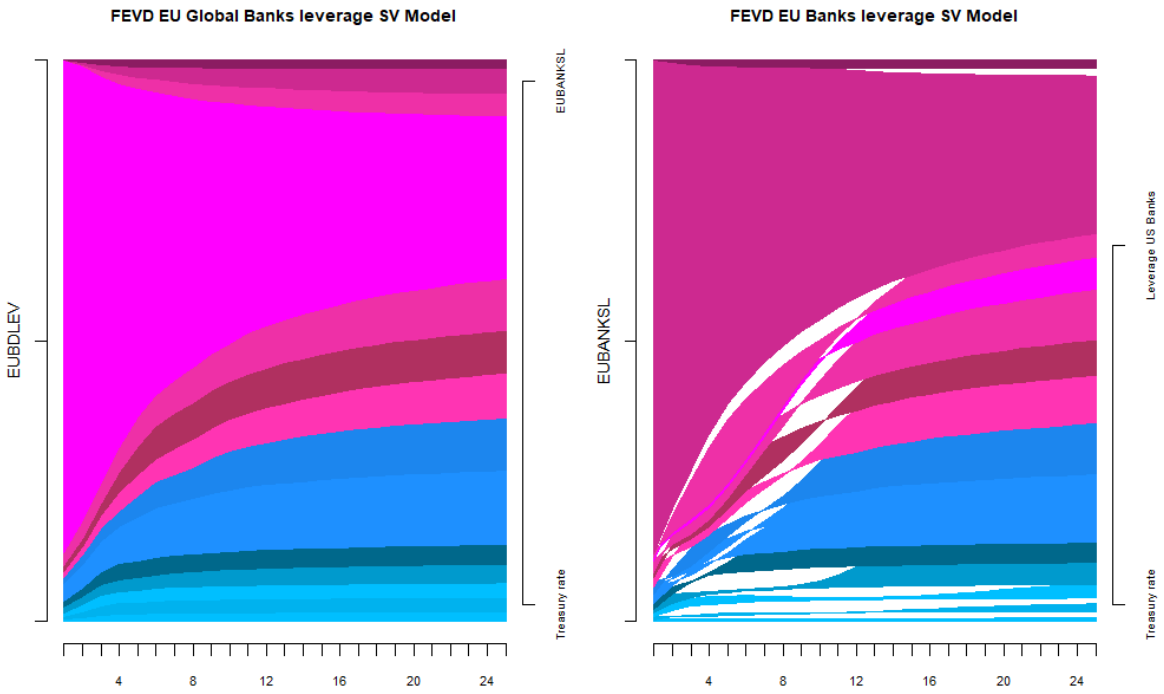

Figure 2: Forecast Error Variance Decomposition (FEVD) Plot of the Stochastic Volatility Bayesian SVAR Model for the Leverage of EU Global Banks and EU Banks

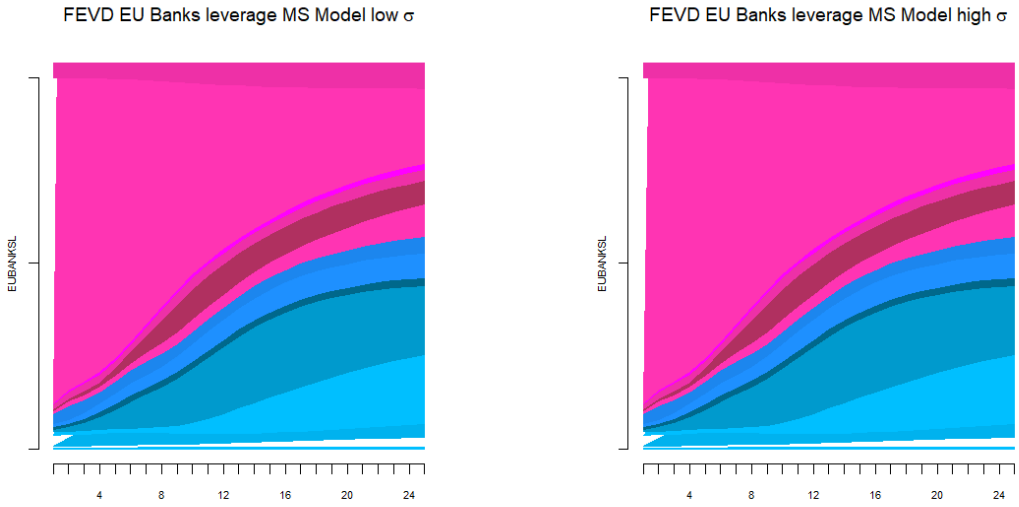

Figure 3: Forecast Error Variance Decomposition (FEVD) Plot of the Markov-Swotching Volatility Bayesian SVAR Model for the Leverage of EU Banks for the Low and High Volatility Regimes

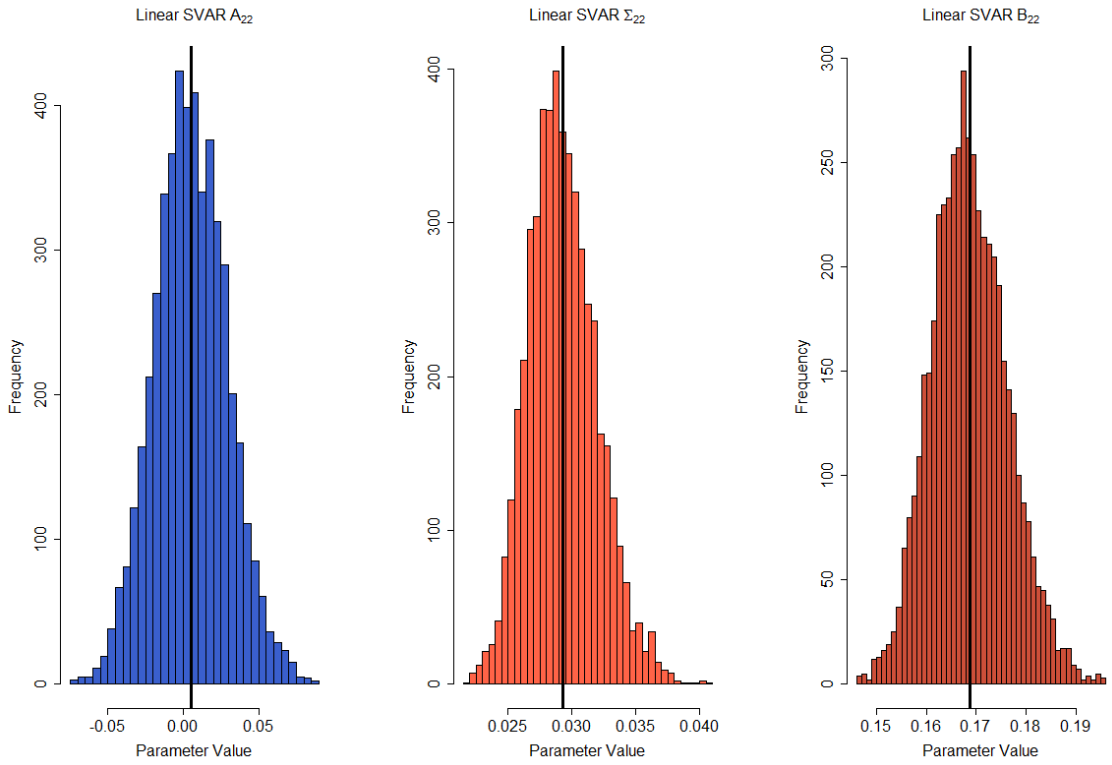

Figure 4: Histogram of the MCMC samples of the Linear SVAR for 5000 draws with 10 thousands iterations of burn-in from the posterior probabilities of the second diagonal matrix element (the 1 Year Treasury Rate) of the autoregressive parameter (in blue), the variance-covariance matrix (in orange), and the contemporaneous effects matrix (in red)

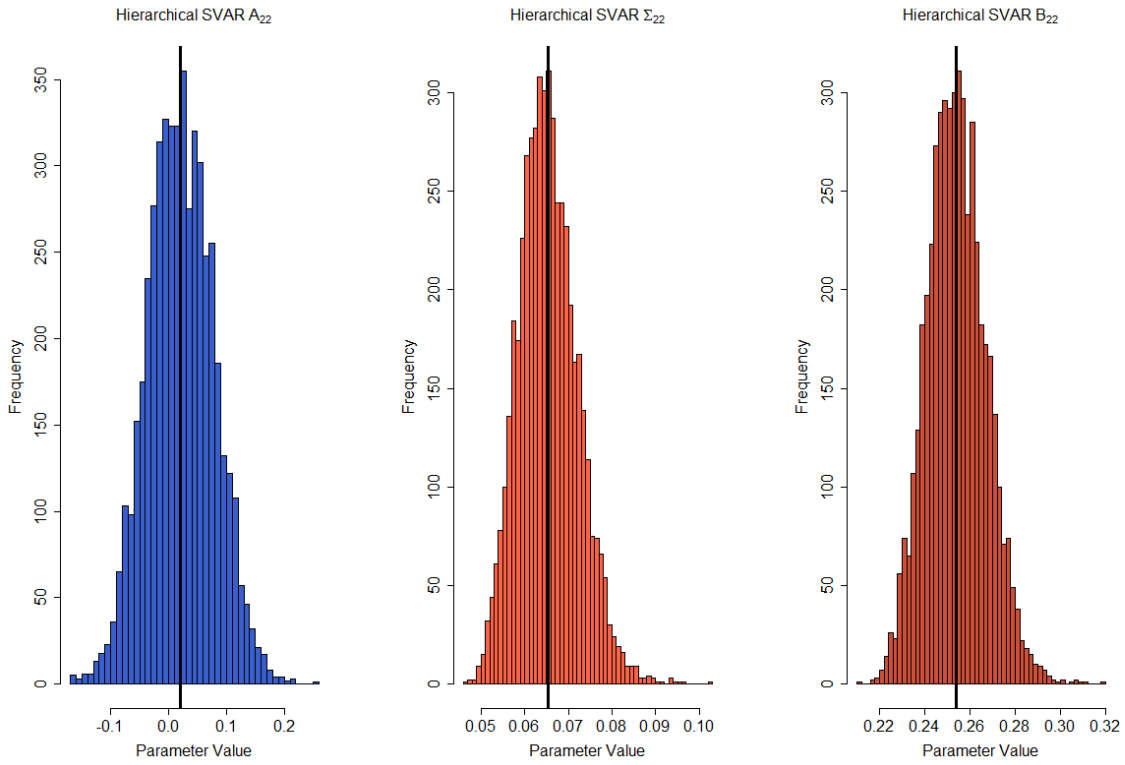

Figure 5: Histogram of the MCMC samples of the Hierarchical SVAR for 5000 draws with 10 thousands iterations of burn-in from the posterior probabilities of the second diagonal matrix element (the 1 Year Treasury Rate) of the autoregressive parameter (in blue), the variance-covariance matrix (in orange), and the contemporaneous effects matrix (in red)

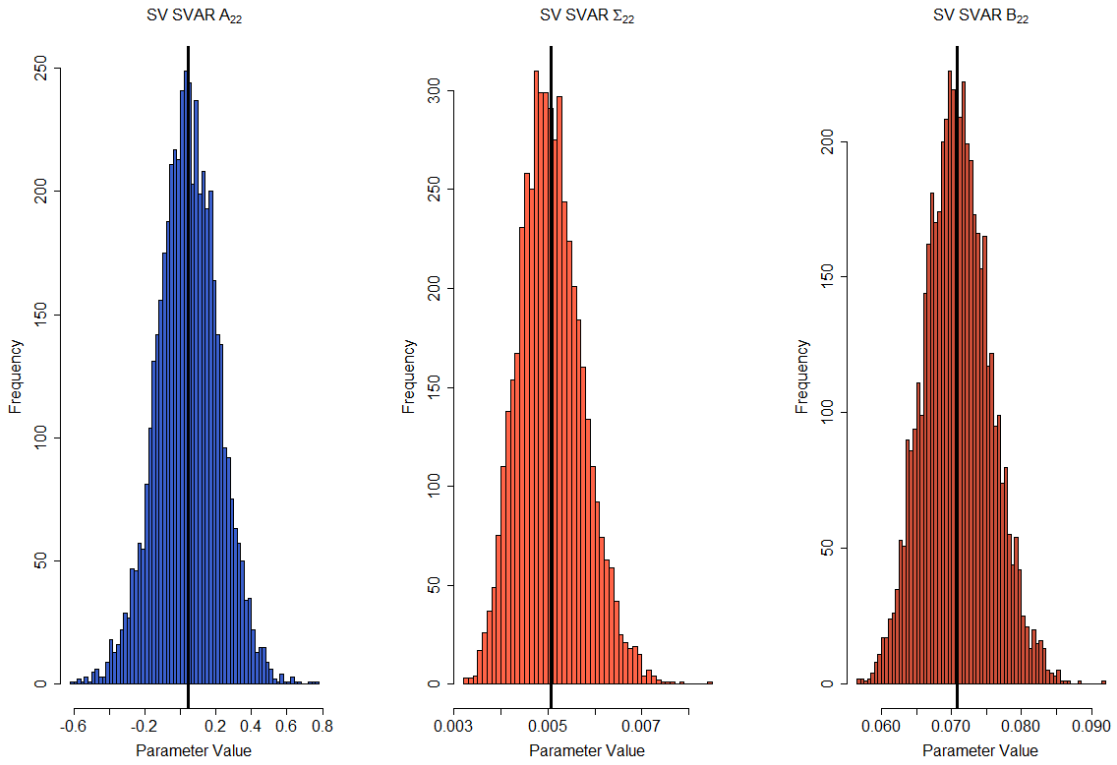

Figure 6: Histogram of the MCMC samples of the Stochastic Volatility SVAR for 5000 draws with 10 thousands iterations of burn-in from the posterior probabilities of the second diagonal matrix element (the 1 Year Treasury Rate) of the autoregressive parameter (in blue), the variance-covariance matrix (in orange), and the contemporaneous effects matrix (in red)

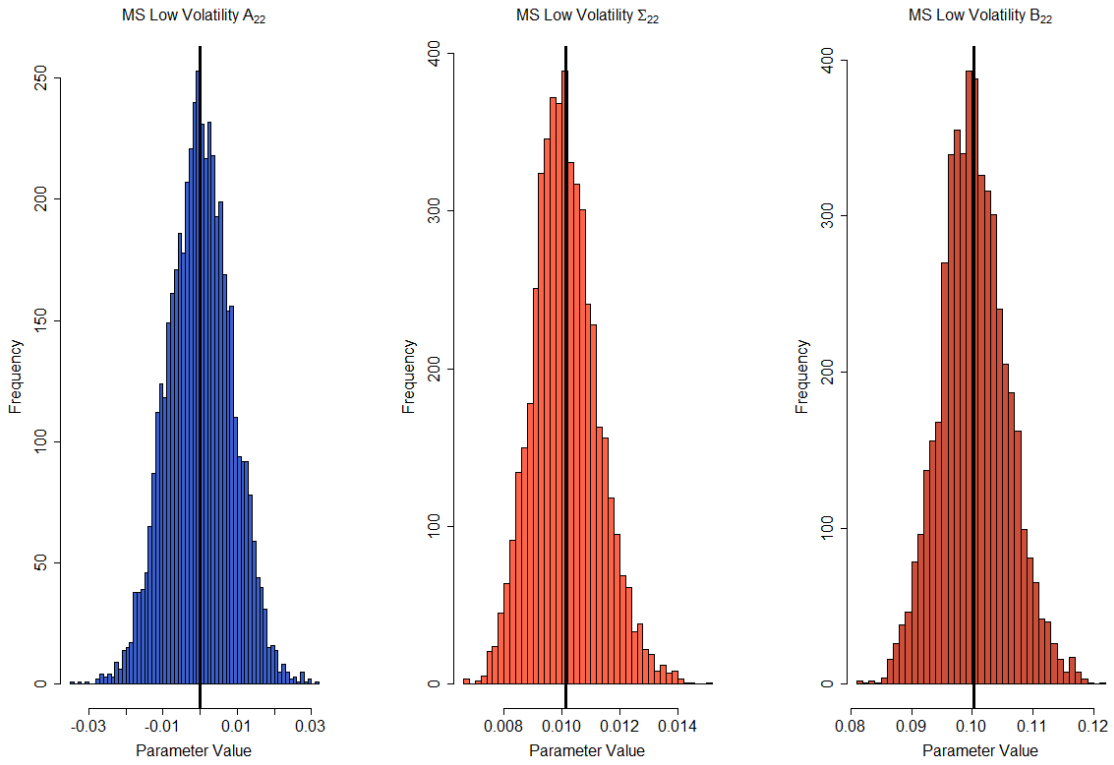

Figure 7: Histogram of the MCMC samples of the Markov-Switching SVAR with Low Volatility for 5000 draws with 10 thousands iterations of burn-in from the posterior probabilities of the second diagonal matrix element (the 1 Year Treasury Rate) of the autoregressive parameter (in blue), the variance-covariance matrix (in orange), and the contemporaneous effects matrix (in red)

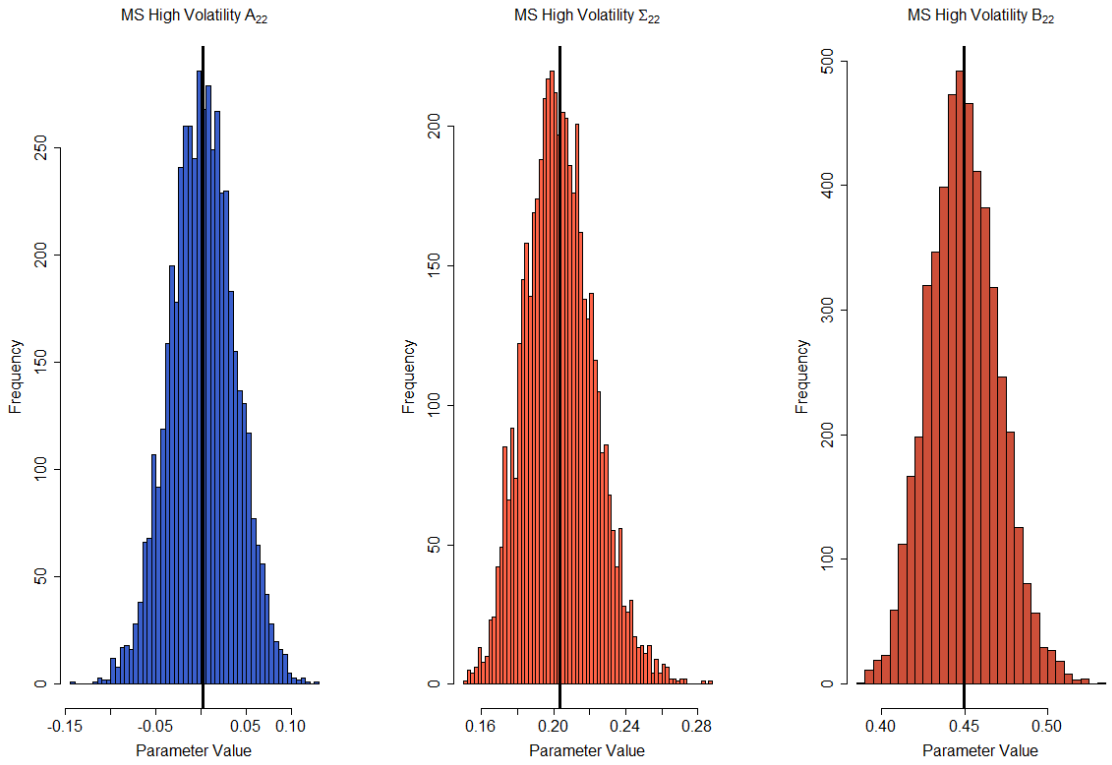

Figure 8: Histogram of the MCMC samples of the Markov-Switching SVAR with High Volatility for 5000 draws with 10 thousands iterations of burn-in from the posterior probabilities of the second diagonal matrix element (the 1 Year Treasury Rate) of the autoregressive parameter (in blue), the variance-covariance matrix (in orange), and the contemporaneous effects matrix (in red)